

**APMP PR-S1 Comparison of
Irradiance Responsivity of UVA Detectors**

Final Report

Gan Xu, Xuebo Huang and Yuanjie Liu

**SPRING Singapore
(Standards, Productivity and Innovation Board)
November 2006**

Contents

1	Introduction.....	6
2	Organization and method of the comparison.....	6
2.1	Method of the comparison	
2.2	Circulation of artifacts and time schedule	
2.3	Measurands	
2.4	Measurement conditions	
2.5	Calculation of relative differences	
3	Preliminary measurements.....	9
3.1	Transfer detectors.....	9
3.1.1	Spectral responsivity	
3.1.2	Spatial uniformity	
3.1.3	Linearity	
3.1.4	Temperature effect	
3.2	UV (365nm) filter.....	13
3.2.1	Spectral transmittance	
3.2.2	Spatial uniformity	
3.3	UV source.....	14
3.3.1	Spectral distribution	
3.3.2	Spatial uniformity of spot at measurement plane	
3.3.3	Stability (short term)	
4	SPRING Singapore's reference standards and traceability.....	17
4.1	Irradiance responsivity of UVA reference standard <i>s(UVA)</i>	
4.2	Irradiance responsivity of UV(365nm) reference standard <i>s(365)</i>	

5	Calibration by SPRING Singapore and uncertainty budget.....	19
5.1	Calibration of $s(UVA)$ of transfer detectors	
5.2	Calibration of $s(365)$ of transfer detectors	
5.3	Uncertainty budget of calibration of transfer detectors	
6	Transfer uncertainty and correction associated with the comparison.....	22
6.1	Drift of $s(UVA)$ and $s(365)$ of transfer detectors	
6.2	Stability of the comparison scale during the period of comparison	
6.3	Transfer uncertainty	
6.4	Temperature effect on transfer detectors	
6.5	Non-linearity of transfer detectors	
6.6	Correction associated with the comparison	
7	Results from national laboratories.....	24
7.1	NMIA (Australia).....	24
7.1.1	Measurement conditions and methods	
7.1.2	Uncertainty budget	
7.1.3	Correction factor and transfer uncertainty	
7.1.4	Comparison with the pilot lab reference value	
7.2	NMIJ (Japan).....	27
7.2.1	Measurement conditions and methods	
7.2.2	Uncertainty budget	
7.2.3	Correction factor and transfer uncertainty	
7.2.4	Comparison with the pilot lab reference value	
7.3	CSIR (South Africa).....	30

7.3.1	Measurement conditions and methods	
7.3.2	Uncertainty budget	
7.3.3	Correction factor and transfer uncertainty	
7.3.4	Comparison with the pilot lab reference value	
7.4	ITRI (Chinese Taipei).....	33
7.4.1	Measurement conditions and methods	
7.4.2	Uncertainty budget	
7.4.3	Correction factor and transfer uncertainty	
7.4.4	Comparison with the pilot lab reference value	
7.5	KRISS (South Korea).....	36
7.5.1	Measurement conditions and methods	
7.5.2	Uncertainty budget	
7.5.3	Correction factor and transfer uncertainty	
7.5.4	Comparison with the pilot lab reference value	
7.6	NIM (China).....	38
7.6.1	Measurement conditions and methods	
7.6.2	Uncertainty budget	
7.6.3	Correction factor and transfer uncertainty	
7.6.4	Comparison with the pilot lab reference value	
8	Overall results.....	42
8.1	Agreement of the laboratories	
8.2	Comparison with a comparison reference value	
8.2.1	Calculation of a comparison reference value	
8.2.2	Uncertainty associated with the comparison reference value	

8.2.3 Unilateral degree of equivalence of NMIs

8.2.4 Bilateral degree of equivalence of NMIs

8.2.5 Statistical checks

9	Conclusions.....	50
10	Acknowledgements.....	50
11	References.....	51
	Appendix 1 Flowchart of data analysis for comparison results.....	52
	Appendix 2 Statistical check for the consistency of the comparison results.....	53

1. Introduction

Broadband UVA radiometers are widely used in a variety of industrial, medical, environmental and other applications. There are so far no internationally agreed standard procedures for the calibration of such radiometers and this has caused unacceptable discrepancies in measurement results.

The aim of this comparison is to assess the equivalence of the standards and techniques used for calibration and measurement of UVA irradiance responsivity of photo-detectors among the participating laboratories.

This comparison was carried out according to a technical protocol ^[11.1] agreed by all participating laboratories and registered as a regional supplementary comparison (APMP PR-S1) with the Key Comparison Data Base (KCDB) of BIPM.

This report describes the principles of the comparison, the preliminary measurements at the pilot laboratory and the results obtained with the participating laboratories.

2. Organization and method of the comparison

2.1 Method of the comparison

The comparison has been carried out through the calibration of a group of two transfer UVA detectors under irradiation of the UV source provided.

The comparison took the form of a star comparison (Fig.2.2.1), carried out in six phases for seven participants. Each phase consists of one laboratory plus the pilot laboratory. The artefacts were first calibrated by the pilot laboratory then sent to the participating laboratory for calibration in each phase. After the participating laboratory completed its calibration, the artefacts were returned to the pilot laboratory for repeat calibration to check the drift.

SPRING Singapore acted as the pilot laboratory. Each laboratory had two and a half months for calibration and transportation. All results were communicated directly to the pilot laboratory within 6 weeks of the completion of the calibration by the participating laboratory.

2.2 Circulation of the artifacts and time schedule

The National Institute of Advanced Industrial Science and Technology of Japan has kindly provided two transfer UVA detectors and a UV source to be used in this comparison. The artefacts (a UV source, a UV 365nm filter, and two UVA detectors) were carefully characterised before being sent to the participating laboratories.

The circulation of the transfer detectors followed the agreed time schedule in Table 2.2.1. Only one laboratory, the MSL(New Zealand), withdrew from the comparison as the measurement time of the comparison clashed with that of CCPR k2.c comparison in MSL.

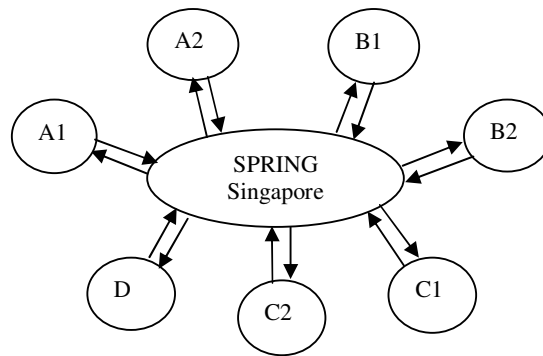


Figure 2.2.1 Diagram of a star comparison

Table 2.2.1 Time schedule for the comparison

Phase	Calibration period	Participating labs
A1	Feb 2003 ~ Apr 2003	NMIA (Australia)
A2	Jun 2003 ~ Aug 2003	NMIJ/AIST (Japan)
B1	Oct 2003 ~ Dec 2003	CSIR (South Africa)
B2	Feb 2004 ~ Apr 2004	ITRI (Chinese Taipei)
C1	May 2004 ~ Jul 2004	KRISS (South Korea)
C2	Sep 2004 ~ Dec 2004	NIM (China)
C2*	Feb 2005 ~ Apr 2005	NIM (China)
D	Cancelled	MSL(New Zealand)

Note: * Repeat calibration was required as anomalous results found in phase C2.

2.3 Measurands

There are two measurands, the narrow band UV (365nm) irradiance responsivity $s(365)$ and the broad band UVA irradiance responsivity $s(UVA)$ of the transfer detectors with respect to the provided UV source.

The narrow band UV (365nm) irradiance responsivity of the transfer detector $s(365)$ is defined as the irradiance responsivity of the detector under the narrow band UV radiation [from the UV source through the UV (365nm) filter provided] at center wavelength 365nm with a bandwidth of approximately 10 nm (FWHM).

$$s(365) = \frac{i}{E(365)} \quad (A \cdot W^{-1} cm^2) \quad (2.3.1)$$

where i is the photocurrent of a transfer detector under the narrow band (centre wavelength: 365nm, bandwidth: $\sim \pm 5$ nm FWHM) UV irradiance, $E(365)$, on the plane of measurement (Fig.2.4.1) produced by the UV source through the UV (365nm) filter:

$$E(365) = \int_0^{\infty} E(\lambda)T(\lambda)d\lambda \quad (W \cdot cm^{-2}) \quad (2.3.2)$$

where $T(\lambda)$ is the spectral transmittance of UV (365nm) filter.

The broad band UVA irradiance responsivity of the transfer detector $s(UVA)$ is defined by:

$$s(UVA) = \frac{i}{E(UVA)} \quad (A \cdot W^{-1} \cdot cm^2) \quad (2.3.3)$$

where i is the photocurrent of the transfer detector under the UVA broad band irradiance, $E(UVA)$, on the plane of measurement (Fig. 2.4.1) produced by the UV source without the UV (365nm) filter. According to CIE definition, UVA irradiance is given by:

$$E(UVA) = \int_{315}^{400} E(\lambda) d\lambda \quad (W \cdot cm^{-2}) \quad (2.3.4)$$

where $E(\lambda)$ is the spectral irradiance produced by the UV source on the plane of measurement.

Note: As the spectral response of an UVA detector is usually not uniform in the UVA (315 – 400 nm) range and may not be zero outside this range, the UVA irradiance responsivity of an UVA detector is source dependent and can only be calibrated against a defined source. The transfer UVA detector and UV source used in this comparison were chosen as they are most commonly used in the industry.

2.4 Measurement conditions

All measurements/calibrations were made under the following conditions:

- a) Overfill condition: the transfer UVA detectors were overfilled by the irradiation of the source;
- b) Angle of incidence on the detector: normal
- c) Incident beam divergence at the detector: $\theta < 5^\circ$ (full angle) (Fig.2.4.1).
- d) Irradiance level:
 - $\leq 0.5 mW/cm^2$ for the narrow band UV (365nm) radiation.
 - $\leq 2 mW/cm^2$ for the broad band UVA radiation.

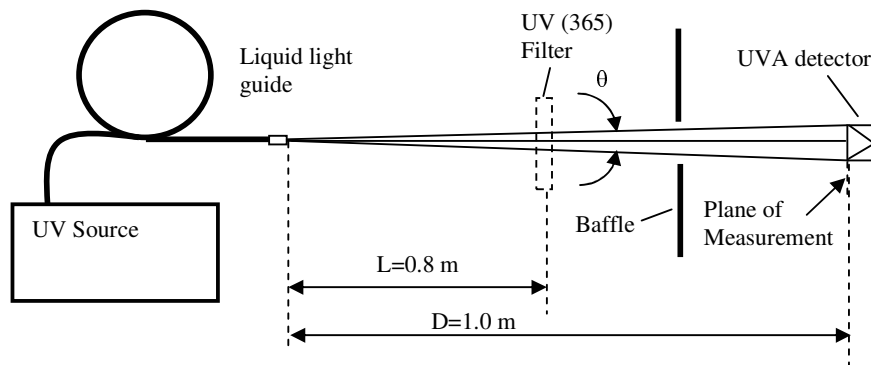


Figure 2.4.1 Block diagram of measurement conditions

- e) Measuring distance: $D=1.0m$ (between the tip of liquid light guide and the plane of measurement as shown in Fig. 2.4.1)

- f) Position of UV (365nm) filter: $L=0.8\text{m}$ as shown in Fig. 2.4.1
- g) Reference plane of UVA detector: as shown in Fig. 2.4.2 (it was placed on the plane of measurement in Fig. 2.4.1).

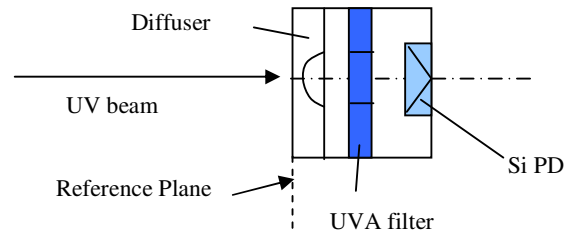


Figure 2.4.2 Block diagram of UVA detector

- h) Alignment: The detector was aligned to the mechanical axis of the liquid light guide.
- i) Warm up time of UV source: At least 40 minutes (allowing the UV source for stabilization).

2.5 Calculation of the relative differences

We denote s_x the irradiance responsivity of a transfer detector calibrated at laboratory x and s_s the irradiance responsivity of the same detector calibrated at SPRING Singapore. The relative difference Δ in the calibrations originating from the participating laboratory and SPRING Singapore is calculated as

$$\Delta = (s_x - s_s) / s_s \quad (2.5.1)$$

As two transfer detectors have been calibrated against the SPRING Singapore reference, which is assumed to be stable, measurements provided by the participating laboratories can be compared to one another via this common reference.

3. Preliminary measurements

It is important to determine the influence of the experimental conditions on the irradiance responsivity of the transfer detectors. This makes it possible to calculate correction factors which can be applied when comparing calibrations made under different experimental conditions, and so estimate the final uncertainty of the comparison.

3.1 Transfer detectors

Two transfer detectors (Manufacturer: International Light, s/n: 7108 and 7112) were used in the comparison. Each consists of a UV enhanced silicon photodiode (Part No: SED033), a UVA broadband filter (Part No: UVA) and a quartz wide eye diffuser (Part No: W).

3.1.1 Spectral responsivity

To assess the suitability of the transfer detector for UVA measurement, the spectral responsivity of one of the transfer detectors with its diffuser removed was measured using the spectral responsivity calibration facility (SRCF, see Fig.5.1.1a) of the pilot lab. The removal of the diffuser was aimed to improve the signal to noise ratio without changing the relative spectral responsivity of the detector.

The radiation from 250nm to 1100nm in 5nm increment was obtained from a xenon lamp (250 – 395nm) and a tungsten lamp (400 – 1100nm) through a double-grating monochromator (3nm bandwidth: 250 - 395nm, 4nm bandwidth: 400 – 1100nm). Detectors were under-filled by the light beam of size $2.0 \times 2.0 \text{ mm}^2$ (250 – 395nm) or $1.3 \times 2.0 \text{ mm}^2$ (400 – 900nm) or $0.67 \times 2.0 \text{ mm}^2$ (905 – 1100nm). The short-circuit photocurrents from the detectors were measured using calibrated current to voltage converters and digital volt meter.

Figure 3.1.1 shows the results of the calibration.

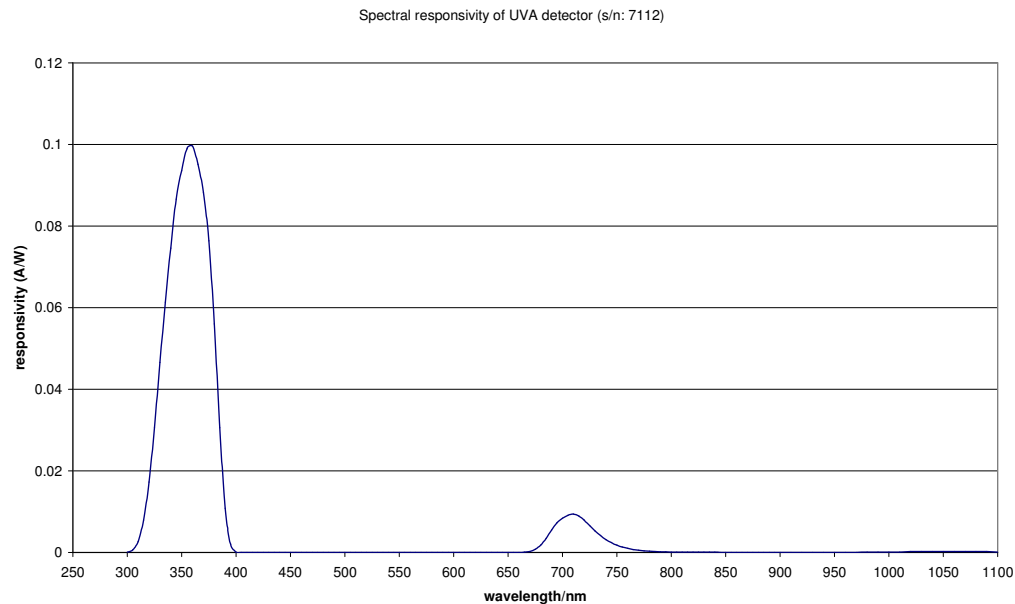


Figure 3.1.1 Spectral responsivity of a traveling detector (s/n: 7112)

As shown in the graph, there is an outer-band response peaking at 710 nm. Its peak value (0.009 A/W) is about 9.1% of the peak value of response at 360 nm (0.0988 A/W) in the UVA range. As there is no output from the calibration UV source at 710nm (see spectrum of calibration UV source in section 3.3.1), the effect of the outer-band response of the transfer detector is very small which can be corrected through dark current measurement.

3.1.2 Spatial uniformity

The spatial uniformity of the transfer detector (with the diffuser attached) was measured by scanning Kr⁺ laser beam of 1.2 mm diameter at 356.4 nm across the area of $20 \times 20 \text{ mm}^2$ with a step of 0.5 mm. The result is shown in Figure 3.1.2 with 10% contours. As there is a diffuser in front of silicon photodiode and UVA filter, the responsivity of transfer detector is spatially non-uniform and decreased from its geometrical center to edge symmetrically. Therefore the alignment of the detector is very important during the calibration.

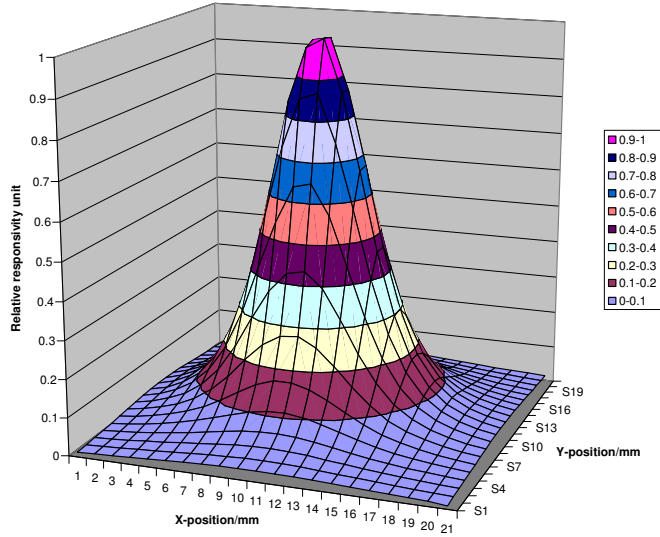


Figure 3.1.2 spatial responsivity distribution of transfer detector with a diffuser

3.1.3 Linearity

The double-aperture method was used to check linearity of the transfer detector. A UV spot curing system (Maker: EXFO) with a liquid light guide was used as a UV source. The output current from the transfer detector was measured by a large dynamic-range current meter (Maker: Melles Griot).

The linearity factor (R_i) at i th irradiance level is calculated as shown in equation (3.1.1):

$$R_i = \frac{S_i(1+2)}{S_i(1) + S_i(2)} \tag{3.1.1}$$

where $S_i(1+2)$ is the output current of the detector under UV incident radiation through two apertures simultaneously and $S_i(1)$ and $S_i(2)$ are the output currents of the detector under the same UV radiation through aperture 1 and aperture 2 respectively.

The linearity correction factor C_n at an output current S_n , relative to a reference current S_k , is then given by equation (3.1.2) ^[11.7].

$$C_n = \frac{\prod_{i=1}^n R_i}{\prod_{i=1}^k R_i} = \frac{R_1 \cdot R_2 \cdot R_3 \cdots R_k \cdots R_n}{R_1 \cdot R_2 \cdot R_3 \cdots R_k} \tag{3.1.2}$$

where R_k is the linearity factor at k th irradiance level corresponding to the reference current S_k and R_n is the linearity factor at n th irradiance level corresponding to the current S_n ($n=1,2,3,\dots$).

The correction factor C_n can be applied to the output S_n to correct the departures from linear behaviors between S_n and a corrected value $S_{n,c}$.

$$S_{nc} = C_n \cdot S_n \tag{3.1.3}$$

The UV irradiances at 365nm measured by most labs were in the range of 0.13 - 0.17 mW/cm² and the UVA irradiances measured by all labs were in the range from 0.6 to 1.0 mW/cm². The experiments showed that the correction factors for $s(365)$ and $s(UVA)$ of the transfer detectors are at the order of ~0.1% as shown in Table 3.1.3.

Table 3.1.3 Correction factor of $s(365)$ and $s(UVA)$ at different irradiance

UV irradiance (mW/cm ²)		Correction factor for $s(365)$	Correction factor for $s(UVA)$
365 nm	0.2 (ref point)	1.000000	
	~0.1	1.000679	
UVA	1.0 (ref point)		1.000000
	~0.5		1.001174

3.1.4 Temperature effect

The relative change of irradiance responsivity of the transfer detector as a function of temperature was determined by measuring output currents of the transfer detector at different temperatures in the range of 21 - 25°C at step of 1°C under the same UV irradiance. The detector was placed in a temperature-controlled housing (Figure 3.1.4). The temperature of the water circulating in the Aluminum block was stabilized by means of a commercial temperature-controlled water bath.

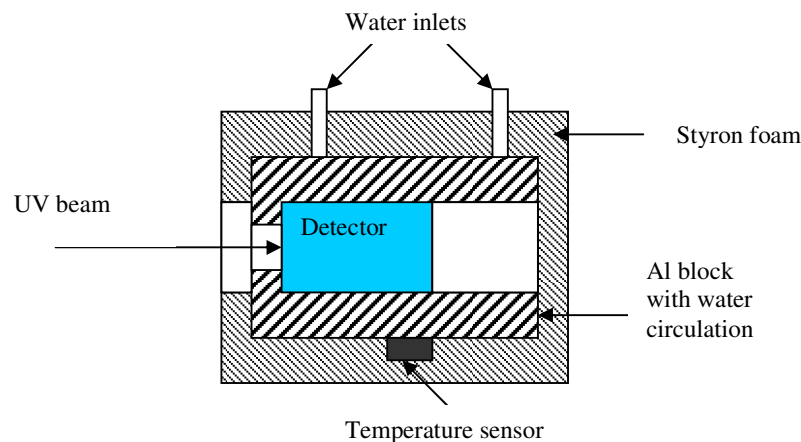


Figure 3.1.4 Temperature controlled housing used to measure the temperature coefficient of the transfer detector.

The linear regression was made for the experimental results. The relative temperature coefficients of responsivity of the transfer detector and the correction factors with respect to 23°C (calibration condition in the pilot lab) for $s(365)$ and $s(UVA)$ were derived as shown in the table 3.1.4a and 3.1.4b.

Table 3.1.4a Relative temperature coefficients of the responsivity of transfer detector

	$\sigma[s(365)](10^{-2} \times ^\circ\text{K}^{-1})$	$\sigma[s(UVA)](10^{-2} \times ^\circ\text{K}^{-1})$
Temperature coefficient	-0.030	-0.135

Note: $\sigma[s(365)]=1/s(365) \times d[s(365)]/dT \times 100\%$ and $\sigma[s(UVA)]= 1/s(UVA) \times d[s(UVA)]/dT \times 100\%$

Table 3.1.4b Correction factors of $s(365)$ and $s(UVA)$ at different temperatures

Temperature (°C)	Correction factor for $s(365)$	Correction factor for $s(UVA)$
21	0.999393	0.997297
21.5	0.999545	0.997971
22	0.999696	0.998647
22.5	0.999848	0.999323
22.6	0.999879	0.999458
23 (ref point)	1.000000	1.000000
24	1.000304	1.001357
25	1.000608	1.002718

3.2 UV (365nm) filter

A UV (365nm) filter was used to produce a narrow band UV radiation. The critical specifications of the filter were:

- Center wavelength : 365nm +/- 1nm
- Bandwidth : 10nm +/- 2nm
- Peak transmittance : >38%
- Effective diameter : >48mm

3.2.1 Spectral transmittance

The spectral transmittance of the filter was measured by a spectrophotometer (Maker: Perkin Elmer, Model: Lambda 900) with a slit width of 1nm and scan step of 0.1 nm in the spectral range from 200 nm to 1100 nm. The beam size on the filter was about 15 x 15 mm². The result of the measurement is shown in Figure 3.2.1.

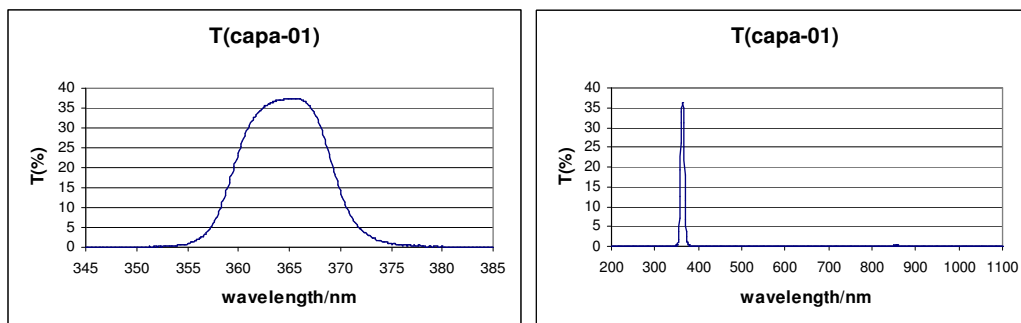


Figure 3.2.1 Spectral transmittance of the UV(365nm) filter shown in two different scanning ranges

3.2.2 Spatial uniformity

The spatial uniformity of the filter was checked at five different positions on the effective area of the filter (see Fig. 3.2.2) using the same spectrophotometer with a slit width of 1nm and scan step of 0.1nm in the spectral range from 350nm to 380nm. The beam size was about 15 x 15 mm². The standard deviation of mean for the readings at five different positions was 0.2%.

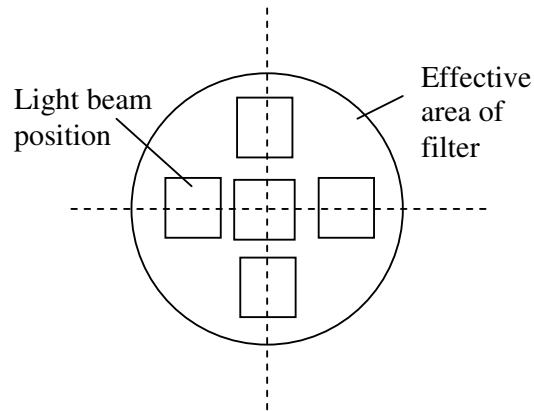


Figure 3.2.2 Light beam positions on the filter surface

3.3 UV source

The UV source used in the comparison was a UV spot curing system (Manufacturer: EFOS Canada Inc., Model: Novacure) with a liquid light guide in which a 100W medium pressure mercury lamp was used.

3.3.1 Spectral distribution

The spectral distribution of the UV source (250 – 1100 nm) was measured using the spectral irradiance calibration facility (SICF, see Figure 5.1.1b) at the pilot lab, by comparison with a group of spectral irradiance reference standard lamps calibrated by NIST. A double-grating monochromator (CVI, DK242) was used as a wavelength selection instrument and a photomultiplier (Hamamatsu, R374) was used as a signal detector. In order to reduce the measurement uncertainty, the scan interval of 1nm was set in the measurement for the fine structure of the mercury spectrum (250-550 nm). But the bandwidth of monochromator had to be increased to 2nm in order to increase the signal to noise ratio.

The measured spectral distribution of the UV source is shown in Figure 3.3.1. The output in the spectral range from 550nm to 1100nm is negligible.

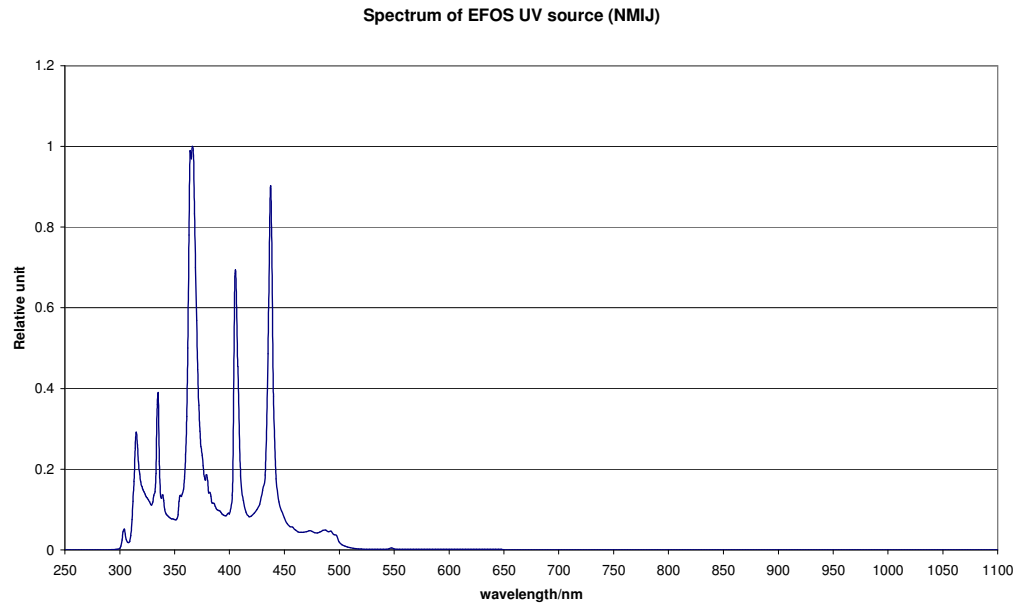


Figure 3.3.1 Spectral distribution of the UV source (EFOS, Model: Novacure)

3.3.2 Spatial uniformity of beam spot at measurement plane

The spatial uniformity of the UV beam spot at the measurement plane (one meter from the tip of the liquid light guide, See Fig. 2.4.1 in Section 2.4) was measured by using a UV detector with 1mm pinhole scanning across the UV spot area of 26 x 26 mm² at a step of 1mm. The result of the measurement is shown in Figure 3.3.2. The spatial distribution of the UV spot may not be the same at different labs because the alignment of UV beam and the position of liquid light guide may vary at different labs. Therefore each lab has done its own uncertainty evaluation for this effect.

The average values of irradiance at different aperture areas (aperture radius from 3mm to 13mm) were calculated out according to the spatial distribution of the UV spot measured in the pilot lab. The maximum deviation of the average irradiances comparing with that of 4 mm aperture radius is about 0.12% under the typical irradiance distribution of UV spot in the pilot lab. Therefore the standard uncertainty caused by the spatial non-uniformity of the UV beam is 0.07% (0.12% divided by 1.732). The test results are shown in table 3.3.2.

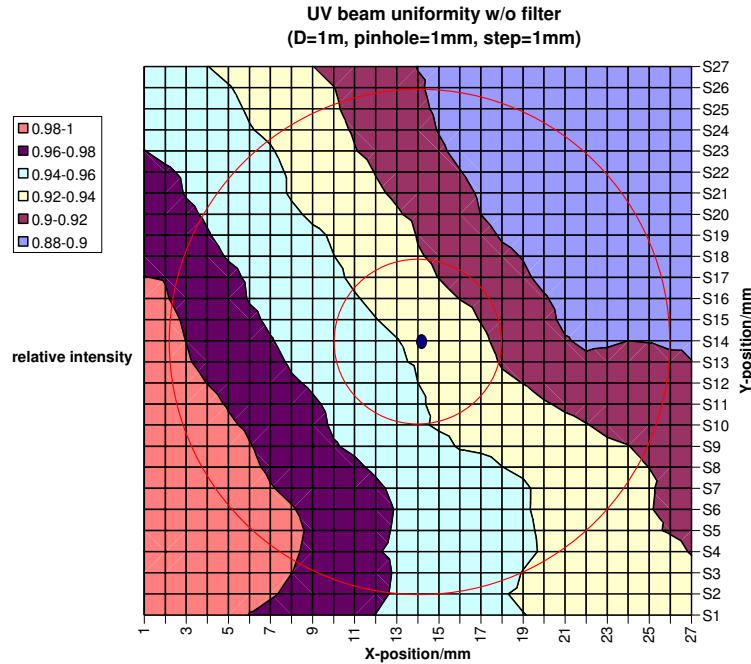


Figure 3.3.2 Spatial uniformity of UV spot (without 365nm filter) at the measurement plane

Table 3.3.2 Average UVA and UV(365nm) irradiance dependence on aperture radius

Aperture radius(mm)	UVA		365nm	
	Average irradiance (relative unit)	Relative difference (%)	Average irradiance (relative unit)	Relative difference (%)
3	1.000685	0.07	1.000892	0.09
4 (ref point)	1.000000	0.00	1.000000	0.00
5	0.999548	-0.05	0.999811	-0.02
6	0.999455	-0.05	1.001096	0.11
7	0.999272	-0.07	1.001243	0.12
8	0.999008	-0.10	1.000795	0.08
9	0.999203	-0.08	1.000942	0.09
10	0.999379	-0.06	1.001089	0.11
11	0.999609	-0.04	1.001045	0.10
12	1.000263	0.03	1.000982	0.10
13	1.000429	0.04	1.000756	0.08

3.3.3 Stability (short terms)

The stability of UV output was tested in a period of 60 minutes after warming up about one hour. The UV output was measured by a UV meter at time interval of one minute. The standard deviation of mean of readings was better than 0.2% as shown in Figure 3.3.3.

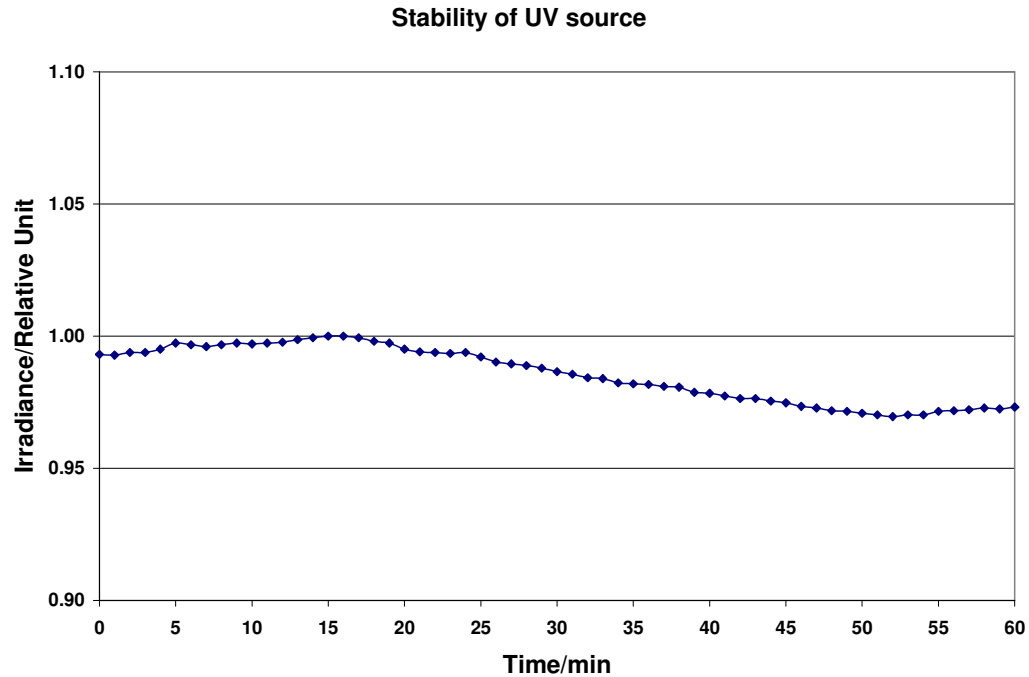


Figure 3.3.3 Short term stability of UV source

4 SPRING Singapore's reference standards and traceability

Two reference standard silicon photodiodes (Model: Hamamatsu S2281, s/n: E458 & E460) were selected as reference standards of the comparison in the pilot lab. Each photodiode was directly calibrated against a silicon trap detector in the spectral range (400-900nm) and the calibration was extended to UV range (250-400nm) with a cavity pyroelectric detector. The trap detector itself was regularly calibrated against the cryogenic radiometer in the pilot lab.

The use of pilot lab's detectors linked to pilot lab's cryogenic radiometer to provide a common reference does not imply s_c is better or more accurate. However they should be stable and maintain over the whole period of the comparison. In fact, the stability of the reference standards was monitored by the pilot lab. The change of $s(365)$ of reference standard silicon photodiode (s/n: E458) is -1.16% and the changes of $s(UVA)$ of reference standard silicon photodiode (s/n: E460) is -0.95% during the whole period of the comparison.

The narrow band UV(365nm) responsivities of two transfer detectors were directly calibrated against one of the reference standard silicon photodiodes (s/n: E458) under narrow band UV(365nm) radiation from the calibration UV source (with 365nm filter). Their broad band (UVA) responsivities were indirectly calibrated against another reference standard silicon photodiode (s/n: E460) under broadband UV source through a working standard UVA detector (s/n: UVA-01, see Fig.4.1 and Section 5). This provides a means of comparing the behavior of the transfer detectors that have been sent to the participating labs with that of the reference standards remaining at the pilot lab, as well as providing a link to the weighted mean of the comparison. The traceability chart of the calibration of transfer detectors in the pilot lab is shown in Figure 4.1.

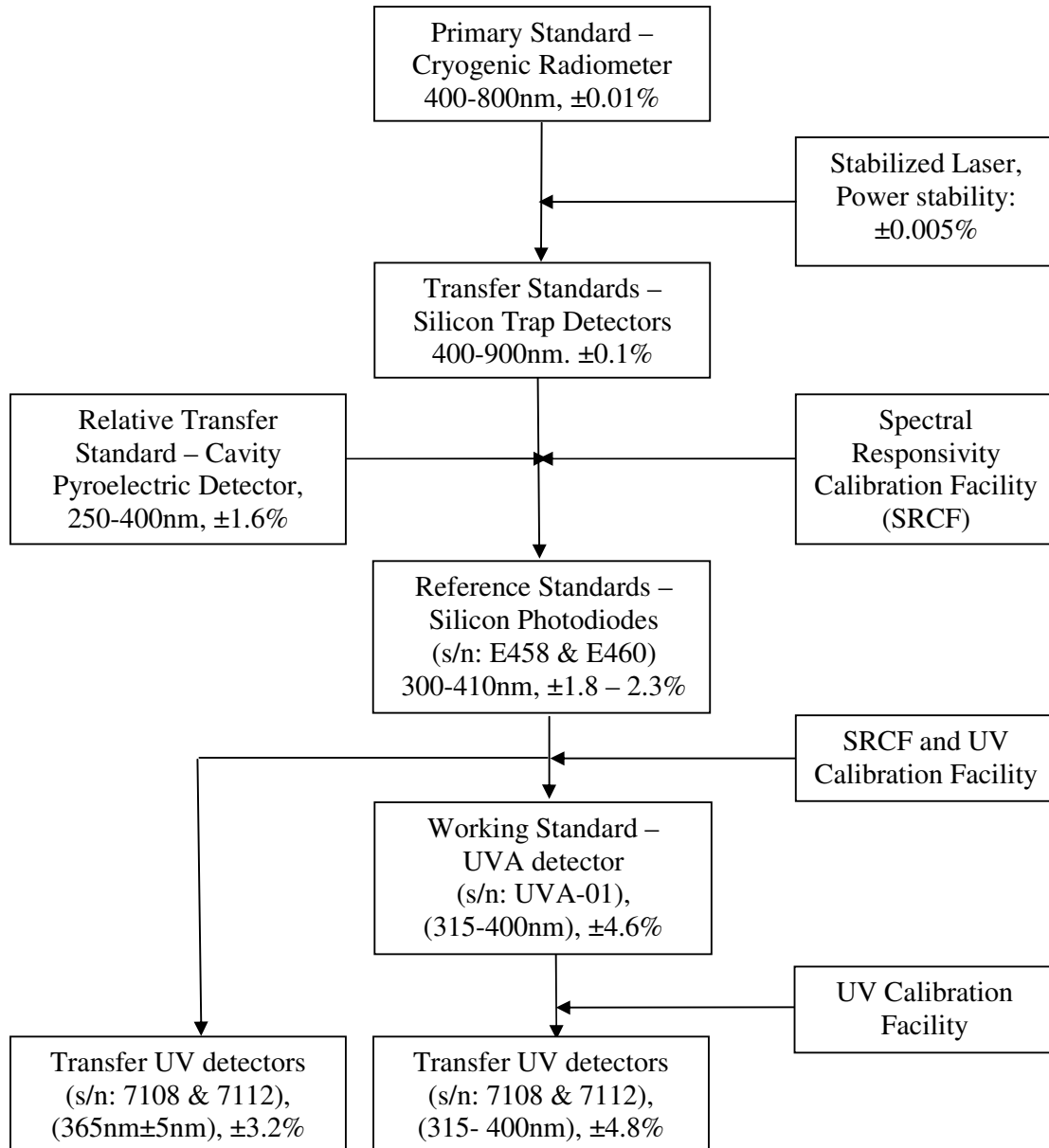


Figure 4.1. Traceability chart for UV detectors calibration (All uncertainty values in the chart refer to expanded uncertainty at a level of confidence ~95% with a coverage factor K=~2)

5 Calibration by SPRING Singapore and uncertainty budget

5.1 Calibration of $s(UVA)$ of transfer detectors

As mentioned in section 4, two transfer detectors were indirectly calibrated against to the reference standard silicon photodiode (s/n: E460) under broadband UV source through a working standard UVA detector (s/n: UVA-01).

5.1.1 Calibration of $s(UVA)$ of working standard detector

From equations (2.3.3) and (2.3.4), the irradiance responsivity of the working standard (W.S) UVA detector against a specified calibration source (denoted by c), $s(UVA)$, is determined by:

$$s(UVA) = \frac{i}{E(UVA)} = \frac{A \int_0^{\infty} s(\lambda) E_c(\lambda) d\lambda}{\int_{315}^{400} E_c(\lambda) d\lambda} \quad (5.1.1)$$

where A is the aperture area of the detector. As $E_c(\lambda)$ appears on both the denominator and numerator in the equation, only relative spectral irradiance (spectral distribution) of the source is required.

In the pilot lab, a UVA detector consisting of a UVA filter, an aperture (8mm in diameter) and a silicon photodiode (Model: 222UV, specially selected with good spatial response) without a diffuser was used as the working standard for calibration. Without a diffuser, the W.S detector has a uniform spatial response, high sensitivity and clear aperture location and diameter. It also has a wide linear dynamic range ($1 \mu\text{W}/\text{cm}^2$ to $100\text{mW}/\text{cm}^2$) which allows it to be calibrated at low irradiance ($100\mu\text{W}/\text{cm}^2$) and then used as a working standard for the calibration of transfer UVA detector at higher irradiance ($2\text{mW}/\text{cm}^2$).

The spectral responsivity of the detector, $s(\lambda)$, is calibrated against a reference standard silicon photodiode in spectral responsivity calibration facility (SRCF) in the Pilot lab (as shown in Fig 5.1.1a).

A 300W xenon arc lamp source (250-400nm), a tungsten strip lamp (400-1100nm) and a double-grating monochromator (CVI, DK242) are used in SRCF as a monochromatic light source. The set-up refers to the requirements of CIE publication No. 64, "Determination of the spectral responsivity of optical radiation detectors". The spectral responsivity of WS UVA detector is calibrated in the range from 250 to 1100nm with interval of 5nm in SRCF. In order to reduce the calculation uncertainty, the interval of spectral responsivity data was fined from 5nm to 1nm through the interpolation method.

The spectral distribution of the UV source is measured in the spectral irradiance calibration facility (SICF) by comparison with a group of spectral irradiance reference standard lamps maintained in the pilot lab (as shown in Figure 5.1.1b).

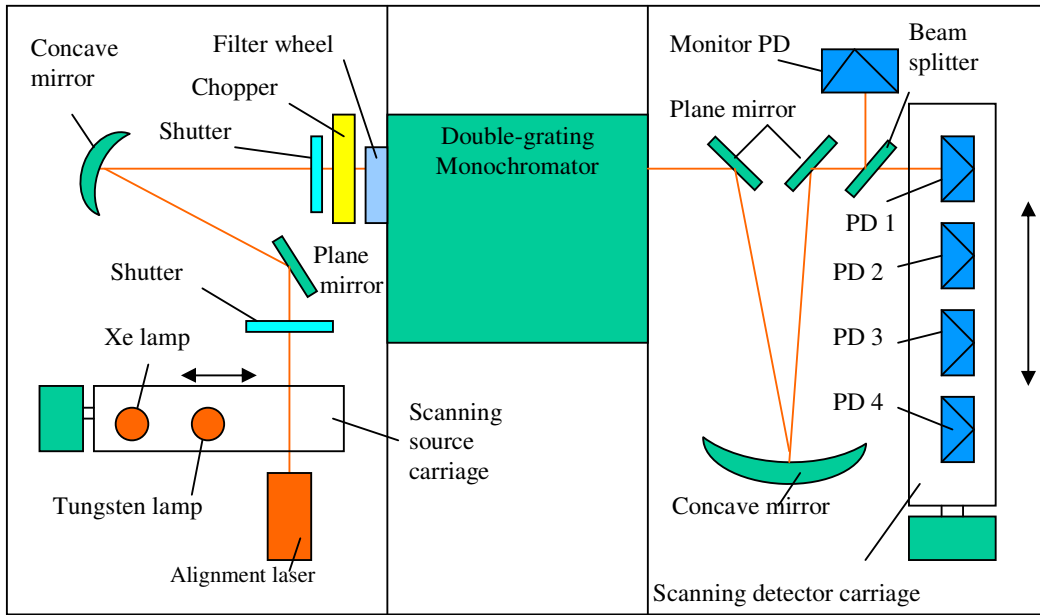


Figure 5.1.1a Block diagram of spectral responsivity calibration facility (SRCF)

A double-grating monochromator (CVI, DK242) is used as a wavelength selection instrument and a photomultiplier (Hamamatsu, R374) as a signal detector. The set-up refers to the requirements of CIE publication No. 63, “The spectroradiometric measurement of light source”. In order to reduce the measurement uncertainty, the scan interval of 1nm was set in the measurement for a fine structure in the mercury spectrum (250-400nm). But the bandwidth of monochromator has to be increased to 2nm in order to increase the signal to noise ratio.

With known aperture area of the detector, the irradiance responsivity of the W.S UVA detector, $s(UVA)$, can then be calculated by using equation (5.1.1).

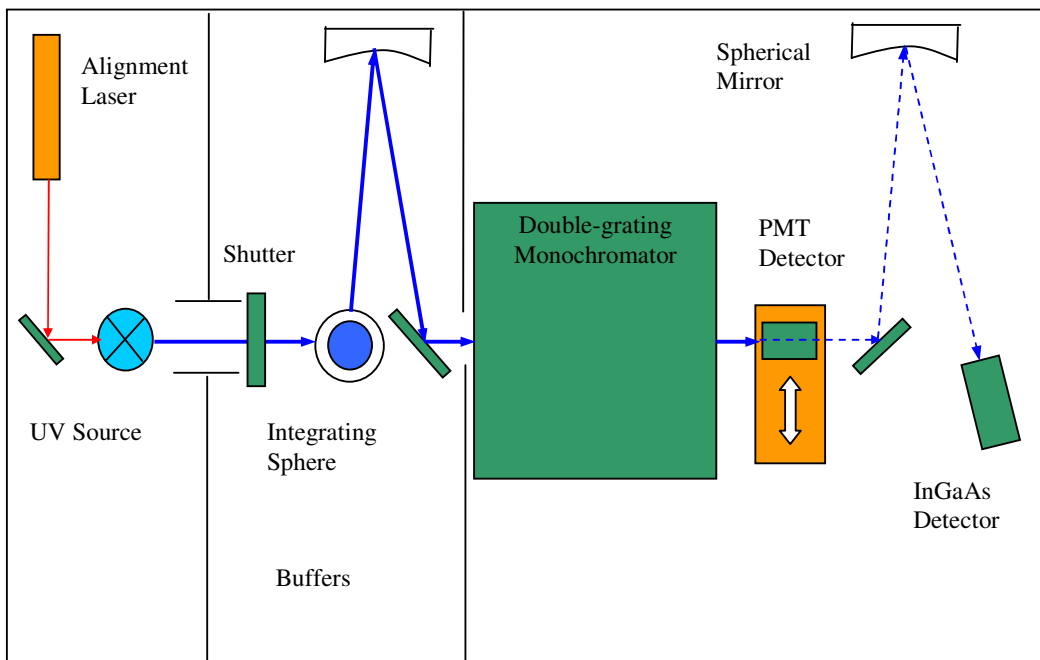


Figure 5.1.1b Block diagram of spectral irradiance calibration facility (SICF)

5.1.2 Calibration of $s_t(UVA)$ of transfer detector

The calibrated W.S UVA detector can then be used to calibrate the transfer UVA detectors under same UV source used in the calibration of the W.S detector. The irradiance responsivity of the transfer detector, $s_t(UVA)$, can then be calculated out by using equation. (5.1.2),

$$s_t(UVA) = s_s(UVA) \frac{i_t}{i_s} \quad (5.1.2)$$

where i_t and i_s are the output photocurrents of the transfer and working standard detectors respectively and $s_s(UVA)$ is the irradiance responsivity of the W.S UVA detector.

The calibration setup is shown in Fig. 2.4.1.

5.2 Calibration of $s(365)$ of transfer detectors

5.2.1 Calibration of $s(365)$ of reference standard detector

Similarly, the irradiance responsivity of UV(365nm) reference standard, $s(365)$, was calculated out by using equation (5.2.1).

$$s(365) = \frac{A \int_0^{\infty} s(\lambda) T(\lambda) E_c(\lambda) d\lambda}{\int_0^{\infty} T(\lambda) E_c(\lambda) d\lambda} \quad (5.2.1)$$

where $T(\lambda)$ is the spectral transmittance of UV (365) filter.

5.2.2 Calibration of $s_t(365)$ of transfer detector

The calibration of $s_t(365)$ of transfer detectors was carried out by comparison with the irradiance responsivity of reference standard, $s_s(365)$, according to equation (5.2.2).

$$s_t(365) = s_s(365) \frac{i_t(365)}{i_s(365)} \quad (5.2.2)$$

where $i_t(365)$ and $i_s(365)$ are the photocurrents of transfer detector and reference standard detector under the comparison UV source.

The calibration setup is shown in Fig. 2.4.1.

5.3 Uncertainty budget of calibration of transfer detectors

The calibration uncertainties have been assessed for both of $s(365)$ and $s(UVA)$ according to the method recommended by International Organization for Standardization (ISO).^[11,8] The major sources of uncertainty have been investigated theoretically and experimentally and the results are shown in table 5.3.1 and table 5.3.2.

Table 5.3.1 Uncertainty budget of calibration of transfer detector, $s(365)$, under narrow band UV (365nm) radiation ($k=1$)

	Source of uncertainty	Value of standard uncertainty (%)
1	Calibration of reference standard detector (s/n:E458)	0.90
2	Drift of reference standard detector	0.33
3	Photocurrent measurement	0.05
4	Reading repeatability of standard detector	0.05
5	Reading repeatability of transfer detector	0.03
6	Alignment and positioning of standard detector	0.45
7	Alignment and positioning of transfer detector	0.22
8	Uncertainty due to uniformity of UV beam and area difference between standard & transfer detectors	1.20
	Combined relative standard uncertainty (%)	1.6

Table 5.3.2 Uncertainty budget of calibration of transfer detector, $s(UVA)$, under broad band UV radiation ($k=1$)

	Source of uncertainty	Value of standard uncertainty (%)
1	Calibration of working standard detector (s/n: UVA-01)	2.30
2	Drift of standard detector	0.27
3	Photocurrent measurement	0.25
4	Reading repeatability of standard detector	0.03
5	Reading repeatability of transfer detector	0.03
6	Alignment and positioning of standard detector	0.45
7	Alignment and positioning of transfer detector	0.22
8	Uncertainty due to uniformity of UV beam and area difference between std & transfer detectors	0.04
	Combined relative standard uncertainty (%)	2.4

6 Transfer uncertainty and correction associated with the comparison

When comparing calibrations from different laboratories, the uncertainty stated by the laboratory should be combined with the uncertainty associated with the comparison (transfer uncertainty) that can contribute to the variability of the results (e.g. the drift of irradiance responsivity of transfer detectors and the stability of the comparison scale during the whole period of the comparison).

The correction should be made for the different measurement conditions between pilot lab and participating lab (e.g. Temperature conditions and UV irradiance levels etc.).

6.1 Drift of $s(UVA)$ and $s(365)$ of transfer detectors

The drifts of $s(UVA)$ and $s(365)$ are determined by the value change of $s(UVA)$ and $s(365)$ before sending the detectors to a participating lab and after receiving them by the pilot lab. The

drift was phase dependent and the value changed from -0.1% to 1.1% for $s(365)$, -0.9% to 0.4% for $s(UVA)$, which should be included in the transfer uncertainty budget.

The drift was usually very small in most phases except for the phase C1 to NIM (China) in August 2004 which changed about -2%. After investigation, we found this unusual large drift was caused by the mould spots developed on the surface of the UVA filter. We believe high humidity and vast temperature change during the transportation of the detector between the labs were responsible for the growth of the mould on the filter surface. In any future comparisons involving filters and photo detectors, proper packing with vapor absorbing material is essential for preventing fungus developing on the surface. Fortunately, this happened in the last phase of the comparison and only NIM's results were affected. After cleaning of the UVA filters, the comparison had been repeated between SPRING Singapore and NIM.

As calibration results of participating labs were compared with average values measured by the pilot lab before sending out and after receiving the transfer detectors, the transfer uncertainty (assuming a rectangular distribution) due to drifts of $s(UVA)$ and $s(365)$, u_{drift} , can be calculated out by using equation (6.1.1).

$$u_{drift} = \frac{|\Delta(drift)|}{2 \cdot \sqrt{3}} \quad (6.1.1)$$

where $\Delta(drift)$ is the drift value.

6.2 Stability of the comparison scale during the period of comparison

The stability of the comparison scale depends on the stability of the reference standards maintained in the pilot lab. The change of $s(365)$ of reference standard silicon photodiode (s/n: E458) is -1.16% and the change of $s(UVA)$ of reference standard silicon photodiode (s/n: E460) is -0.95% during the whole period of the comparison. The standard uncertainty (assuming a rectangular distribution) due to those changes, u_{stab} , can be calculated out by using equation (6.2.1).

$$u_{stab} = \frac{|\Delta(change)|}{2\sqrt{3}} \quad (6.2.1)$$

where $\Delta(change)$ is the change (in percentage) of $s(365)$ or $s(UVA)$ of reference standard silicon photodiodes during the whole period of the comparison.

In this comparison, the standard uncertainty due to stability of the SPRING reference standard, u_{stab} , are 0.33% and 0.27% for $s(365)$ and $s(UVA)$ respectively. To take into account the change of $s(365)$ and $s(UVA)$ of reference standard, the $s(365)$ and $s(UVA)$ of transfer detector should be corrected by using equation (6.2.2).

$$s_c = s \times CF \quad (6.2.2)$$

where s and s_c are the irradiance responsivity values of transfer detector before and after correction for the change of reference standard. The correction factor (CF) is defined by using equation (6.2.3).

$$CF = 1 + \frac{\Delta(\text{change})}{2 \times 100} \quad (6.2.3)$$

CF values are 0.9942 and 0.99525 for $s(365)$ and $s(UVA)$ of transfer detectors respectively.

6.3 Transfer uncertainty

The transfer uncertainty, u_T , of each participant is the combination of u_{drift} and u_{stab} and can be calculated by using equation (6.3.1).

$$u_T = \sqrt{u_{drift}^2 + u_{stab}^2} \quad (6.3.1)$$

6.4 Temperature effect of transfer detectors

The correction should be done for the calibration results of participants at different temperatures (21 – 25°C). The correction factors at different temperatures against the reference temperature (23°C) can be referred to table 3.1.4b.

6.5 Non-linearity of transfer detectors

As the calibration in each lab was done at different irradiance levels (0.13- 0.17 mW/cm²) for 365nm and (0.6- 1.0 mW/cm²) for UVA respectively, the correction can be done according to table 3.1.3.

6.6 Correction associated with the comparison

Appendix 1 shows the flow chart for the calculation of relative difference of $s(365)$ or $s(UVA)$ of transfer detectors between pilot lab and participating lab.

7 Results from national laboratories

7.1. NMIA (Australia)

7.1.1. Measurement conditions and methods

a) Measurement Conditions

- Spectroradiometer type: McPherson 285 double grating 0.5m monochromator
- Standards used: Silicon photodiodes for $s(365)$ and $s(UVA)$
- Irradiance level: 0.16 mW/cm² (365±5 nm), 1.04 mW/cm² (UVA)
- Room temperature: 21.5 ± 0.5 °C
- Aperture diameter of reference detectors: Φ6mm (Reference Si photodiode)

b) Method used to determine $s(UVA)$ of transfer detector

$s(UVA)$ of transfer detector was calibrated by comparison with NMIA reference standard UVA radiometer against the comparison UV source. $s(UVA)$ of the UVA

radiometer was calculated out according to equation (5.1.1) through measurements of relative spectral irradiance of the UV source and absolute spectral responsivity of the UVA radiometer.

c) Method used to determine $s(365)$ of transfer detectors

$s(365)$ of transfer detector was calibrated by comparison with three NMIA silicon photodiodes against the comparison UV source with a UV (365nm) filter.

7.1.2. Uncertainty budget

Table 7.1.2a and 7.1.2b are the uncertainty budgets of calibration of transfer detectors (s/n : 7108 and 7112) under the narrow band (365nm) and broad band (UVA) irradiance ($k=1$).

Table 7.1.2a Uncertainty budget of $s(365)$ of transfer detectors

	Source of uncertainty	Value of standard uncertainty (%)
1	Uncertainty in calibration of reference Si photodiode at 365nm	0.14
2	Uncertainty in correction of response for 10nm SBW from source	0.05
3	Uncertainty in photocurrent measurement	0.02
4	Uncertainty in transfer to test radiometers including lamp instability	0.01
5	Uncertainty in alignment and distance reference detectors	0.05
6	Uncertainty in alignment and distance test detectors	0.05
7	Uncertainty in correction for area difference and field non-uniformity between reference Si diode aperture and reference UV radiometer	1.0
	Combined relative standard uncertainty	1.1

Table 7.1.2b Uncertainty budget of $s(UVA)$ of transfer detectors

	Source of uncertainty	Value of standard uncertainty (%)	
		7108	7112
1	Uncertainty in calibration of reference radiometer at 365nm	0.14	0.14
2	Uncertainty in calculation of UVA response from Novacure lamp	0.17	0.17
3	Uncertainty in photocurrent measurement	0.02	0.02
4	Uncertainty in transfer to test radiometers including lamp instability	0.04	0.25
5	Uncertainty in alignment and distance reference detectors	0.05	0.05
6	Uncertainty in alignment and distance test detectors	0.05	0.05
7	Uncertainty in correction for area difference and field non-uniformity between reference Si diode aperture and reference UV radiometer	0.05	0.05
	Combined relative standard uncertainty	0.24	0.34

7.1.3. Correction factors and transfer uncertainty

a) Correction factors

- Room temperature: 21.5+/-0.5°C. The correction factors are 0.999545 for $s(365)$ and 0.997971 for $s(UVA)$.
- Irradiance levels measured in NMIA are 0.16 mW/cm² (365nm) and 1.04 mW/cm² (UVA) which are similar with those in the pilot lab. Therefore no correction has been applied.

The correction for the different measurement condition is summarized in the table 7.1.3a.

Table 7.1.3a Correction for different measurement conditions with pilot lab

	$s(365)$		$s(UVA)$	
Correction factor	0.999545		0.997971	
Detector s/n	7108	7112	7108	7112
Before correction	0.00743	0.00766	0.00557	0.00573
After correction	0.007427	0.007657	0.005559	0.005718

b) Transfer uncertainty

The drifts of $s(365)$ and $s(UVA)$ of transfer detectors before and after measurement in NMIA are -0.13% and -0.87% respectively. The standard uncertainties due to drifts of $s(365)$ and $s(UVA)$ of transfer detectors, u_{drift} , are 0.04% (365nm) and 0.25% (UVA) respectively according to equation (6.1.1). The standard uncertainties due to stability of the comparison scale, u_{stab} , are 0.33% (365nm) and 0.27% (UVA) according to equation (6.2.1). The transfer uncertainties, u_T , are 0.33% (365nm) and 0.37% (UVA) according to equation (6.3.1). The transfer uncertainties of NMIA's results are summarized in Table 7.1.3b.

Table 7.1.3b Transfer uncertainty of NMIA's results

	365nm	UVA
$u_{drift}(\%)$	0.04	0.25
$u_{stab}(\%)$	0.33	0.27
$u_T(\%)$	0.33	0.37

7.1.4. Comparison with the pilot lab reference value

The corrected relative difference Δ in the comparison was calculated for each detector, according to the equation (2.5.1) in the section 2.5, as shown in table 7.1.4a.

Table 7.1.4a Relative difference in the comparison $(s_{NMIA} - s_{SPRING})/s_{SPRING}$

Detector (s/n)	$\Delta_I(\%),365nm$	$\Delta_I(\%),UVA$
7108	+0.34	-0.53
7112	+0.87	+0.19
Average	+0.60	-0.17

The combined relative standard uncertainty of the comparison, $u(\Delta_I)$, is calculated according to following formula (7.1.4) and summarized in table 7.1.4b.

$$u^2(\Delta_I) = u_{rel}^2(\Delta_I) + u_T^2(\Delta_I) \quad (7.1.4)$$

$u_{rel}(\Delta_i)$: Total relative uncertainty of $s(365)$ or $s(UVA)$ reported by the participant.

$u_T(\Delta_i)$: The transfer uncertainty due to drift of transfer detectors and the stability of the comparison scale.

Table 7.1.4b Combined relative standard uncertainty of NMIA results ($k=1$)

	365nm	UVA
$u_{rel}(\Delta_i), \%$	1.10	0.29*
$u_T(\Delta_i), \%$	0.33	0.37
$u(\Delta_i), \%$	1.15	0.47

* The value is the average of $u(7108)$ and $u(7112)$ provided by NMIA.

7.2. NMIJ (Japan)

7.2.1. Measurement conditions and methods

a) Measurement Conditions

- Spectroradiometer type: JASCO double grating 0.25m, F4.3. 600/mm
- Standards used: Trap detector for $s(365)$, standard lamps for $s(UVA)$
- Irradiance level: 0.14 mW/cm² (365±5 nm), 0.85 mW/cm² (UVA)
- Room temperature: 22.6 ± 1 °C
- Aperture diameter of standard detector: Φ8mm (0.5cm²) (trap detector)

b) Method used to determine $s(UVA)$ of transfer detector

$s(UVA)$ of transfer detector was calibrated by measuring the output signal of the transfer detector against UVA irradiance of the comparison UV source whose spectral irradiance was calibrated by reference standard spectral irradiance lamps maintained in NMIJ.

c) Method used to determine $s(365)$ of transfer detector

$s(365)$ of transfer detector was calibrated by comparison with a reference standard silicon trap detector whose irradiance responsivity at 365nm, s_T , was calculated based on the spectral responsivity of the trap detector, $s_T(\lambda)$, and the relative spectral irradiance of the comparison UV source with a UV(365nm) filter, $E_c(\lambda)$, and the entrance aperture area, A, of trap detector according to equation (7.2.1) below:

$$s_T = \frac{A \int_{350}^{380} s_T(\lambda) E_c(\lambda) d\lambda}{\int_{350}^{380} E_c(\lambda) d\lambda} \quad (7.2.1)$$

7.2.2. Uncertainty budget

Tables 7.2.2a and 7.2.2b are the uncertainty budgets of calibration of transfer detectors under narrow band UV (365nm) and broad band UVA irradiance ($k=1$).

Table 7.2.2a Uncertainty budget of $s(365)$ of transfer detectors ($k=1$)

	Source of uncertainty	Type	Value (%) ($k=1$)	Probability distribution	Divisor	Value of standard uncertainty (%) ($k=1$)
1	Spectral responsivity calibration of standard detector	B	0.8	normal	1.0	0.8
2	Determination of average irradiance responsivity	B	1.5	rectangular	$3^{1/2}$	0.9
3	Photocurrent measurement	B	0.2	normal	1.0	0.2
4	Reading repeatability of standard detector	A	0.01	normal	1.0	0.01
5	Reading repeatability of test detector	A	0.1	normal	1.0	0.1
6	Alignment and positioning of standard detector ¹⁾	B	1.0	rectangular	$3^{1/2}$	0.6
7	Alignment and positioning of test detector ¹⁾	B	1.0	rectangular	$3^{1/2}$	0.6
8	Instability of UV source	B	1.0	rectangular	$3^{1/2}$	0.6
	Combined relative standard uncertainty (%)					1.6

1) Due to non-uniformity of UV beam and area difference between standard & test detectors.

Table 7.2.2b. Uncertainty budget of $s(UVA)$ of transfer detectors ($k=1$)

	Source of uncertainty	Type	Value (%) ($k=1$)	Probability distribution	Divisor	Value of standard uncertainty (%) ($k=1$)
1	Calibration of spectral irradiance standard lamp	B	2.4	normal	1.0	2.4
2	Determination of wavelength-integrated irradiance	B	2.0	rectangular	$3^{1/2}$	1.2
3	Photocurrent measurement	B	0.2	normal	1.0	0.2
4	Reading repeatability of standard detector	A	0.01	normal	1.0	0.01
5	Reading repeatability of test detector	A	0.1	normal	1.0	0.1
6	Alignment and positioning of standard detector ¹⁾	B	1.0	rectangular	$3^{1/2}$	0.6
7	Alignment and positioning of test detector ¹⁾	B	1.0	rectangular	$3^{1/2}$	0.6
8	Instability of UV source	B	2.5	rectangular	$3^{1/2}$	1.4
	Combined relative standard uncertainty (%)					3.2

1) Due to non-uniformity of UV beam and area difference of observation between standard & test detectors.

7.2.3. Correction factors and transfer uncertainty

a) Correction

- Temperature: 22.6+/-1°C. The correction factors are 0.999879 for $s(365)$ and 0.999458 for $s(UVA)$.
- Irradiance levels measured in NMIJ are 0.14mW/cm² (365nm) and 0.85mW/cm² (UVA). The irradiance levels are similar with those in the pilot lab and no correction has been applied.

The correction for the different measurement condition is summarized in the table 7.2.3a.

Table 7.2.3a Correction for different measurement conditions with pilot lab

Correction factor	$s(365)$		$s(UVA)$	
	0.999879		0.999458	
Detector s/n	7108	7112	7108	7112
Before correction	0.00756	0.00776	0.00573	0.00585
After correction	0.007559	0.007759	0.005727	0.005847

b) Transfer uncertainty

Drifts of $s(365)$ and $s(UVA)$ of transfer detectors before and after measurement in NMIJ are -0.34% and 0.35% respectively. The standard uncertainties due to drifts of $s(365)$ and $s(UVA)$ of transfer detectors, u_{drift} , are 0.10% according to equation (6.1.1). The standard uncertainties due to stability of the comparison scale, u_{stab} , are 0.33% (365nm) and 0.27% (UVA) according to equation (6.2.1). The transfer uncertainties, u_T , are 0.34% (365nm) and 0.29% (UVA) according to equation (6.3.1). The transfer uncertainties of NMIJ's results are summarized in Table 7.2.3b.

Table 7.2.3b Transfer uncertainty of NMIJ's results

	365nm	UVA
$u_{drift} (\%)$	0.10	0.10
$u_{stab} (\%)$	0.33	0.27
$u_T (\%)$	0.34	0.29

7.2.4 Comparison with the pilot lab reference value

The corrected relative difference Δ in the comparison was calculated for each detector, according to the equation (5.2.1) in the section 5.2, as shown in table 7.2.4a.

Table 7.2.4a Relative difference in the comparison $(s_{NMIJ} - s_{SPRING})/s_{SPRING}$

Detector (s/n)	$\Delta_2 (\%), 365nm$	$\Delta_2 (\%), UVA$
7108	+2.61	+2.85
7112	+2.22	+2.62
Average	+2.41	+2.73

The combined relative standard uncertainty of the comparison $u(\Delta_2)$ is calculated according to following formula (7.2.4) and summarized in the table 7.2.4b.

$$u^2(\Delta_2) = u_{rel}^2(\Delta_2) + u_T^2(\Delta_2) \quad (7.2.4)$$

$u_{rel}(\Delta_i)$: Total relative uncertainty of $s(365)$ or $s(UVA)$ reported by the participant.

$u_T(\Delta_i)$: The transfer uncertainty due to drift of transfer detectors and the stability of the comparison scale.

Table 7.2.4b Combined relative standard uncertainty of NMIJ results ($k=1$)

	365nm	UVA
$u_{rel}(\Delta_2), \%$	1.6	3.2
$u_T(\Delta_2), \%$	0.34	0.29
$u(\Delta_2), \%$	1.64	3.21

7.3. CSIR (South Africa)

7.3.1 Measurement conditions and methods

a) Measurement conditions

- Spectroradiometer type: Jobin Yvon H10D double grating 1200/mm + integrating sphere
- Standards used: Standard spectral irradiance lamps for $s(UVA)$ and absolute radiometer for $s(365)$
- Irradiance level: 0.15-0.35 mW/cm² (365±5 nm), 0.97 mW/cm² (UVA)
- Room temperature: 25 ± 2 °C
- Aperture diameter of standard detector: Φ11.3mm (1.0cm²) (Absolute radiometer), Φ10mm (0.75cm²) (Monochromator entrance aperture)

b) Method used to determine $s(UVA)$ of transfer detector

$s(UVA)$ of transfer detector was calibrated by measuring the output signal of the transfer detector against UVA irradiance of the comparison UV source whose spectral irradiance was calibrated by reference standard spectral irradiance lamps maintained in CSIR. An additional calibration for $s(UVA)$ of the transfer detectors was obtained by comparison to the absolute radiometer using a stable Xe arc lamp plus UVA filter.

c) Method used to determine $s(365)$ of transfer detector

$s(365)$ of transfer detectors were calibrated by direct comparison to an absolute radiometer (irradiance mode) using the comparison UV source plus UV(365nm) filter.

7.3.2 Uncertainty budget

Table 7.3.2a and 7.3.2b are the uncertainty budgets of calibration of transfer detector under narrow band UV (365nm) and broad band UVA irradiance ($k=1$).

Table 7.3.2a Uncertainty budget of $s(365)$ of transfer detectors

	Source of uncertainty	Value of standard uncertainty (%)
1	Calibration of standard detector	1
2	Photocurrent measurement	0.1
3	Reading repeatability of standard detector	0.5
4	Reading repeatability of test detector	0.2
5	Alignment and positioning of standard detector	2
6	Alignment and positioning of test detector	1
7	Uncertainty due to uniformity of UV beam and area difference between standard & test detectors	3
8	Lamp stability	0.5
	Combined relative standard uncertainty (%)	4.0

Note: this calibration was done using two different source combinations which gave different results. The combined relative standard uncertainty for the end result is estimated to be about 4 and 6% respectively. The standard detector aperture was 1 cm^2 . The non-uniformity induced uncertainty was less when using a Xe source + UVA interference filter for detector calibration.

Table 7.3.2b Uncertainty budget of $s(UVA)$ of transfer detectors

	Source of uncertainty	Value of standard uncertainty (%)
1	Calibration of lamp for UVA irradiance	3.7
2	Photocurrent measurement	0.1
3	Reading repeatability of standard detector	NA
4	Reading repeatability of test detector	0.2
5	Alignment and positioning of standard detector	NA
6	Alignment and positioning of test detector	4
7	Uncertainty due to uniformity of UV beam	4
8	Lamp repeatability between calibration and detector measurement	3
	Combined relative standard uncertainty (%)	7.5

Note 1: the detector was calibrated vs the traveling lamp which was calibrated for spectral irradiance. The difference in aperture size between detector and entrance sphere of the monochromator caused an extra uncertainty due to the beam non-uniformity.

Note 2: CSIR has increased its data in the uncertainty budget for $s(UVA)$ from 4% to 7.5% on 26 September 2005.

7.3.3 Correction factors and transfer uncertainty

a) Correction

- Temperature: $25\pm 2^\circ\text{C}$. The correction factors are 1.000608 for $s(365)$ and 1.002718 for $s(UVA)$.

- Irradiance levels measured in CSIR are 0.15 mW/cm² (365nm) and 0.97mW/cm² (UVA). The UVA irradiance levels are similar with those of pilot lab and no correction has been applied.

The correction for the different measurement condition is summarized in the table 7.3.3a.

Table 7.3.3a Correction for different measurement conditions with pilot lab

	<i>s</i> (365)		<i>s</i> (UVA)	
Correction factor	1.000608		1.002718	
Detector s/n	7108	7112	7108	7112
Before correction	0.0078	0.0081	0.0060	0.0062
After correction	0.00780	0.00810	0.00602	0.00622

b) Transfer uncertainty

Drifts of *s*(365) and *s*(UVA) of transfer detectors before and after measurement in CSIR are - 0.26% and 0.26% respectively. The standard uncertainties due to drifts of *s*(365) and *s*(UVA) of transfer detectors, u_{drift} , are 0.08% according to equation (6.1.1). The standard uncertainties due to stability of the comparison scale, u_{stab} , are 0.33% (365nm) and 0.27% (UVA) according to equation (6.2.1). The transfer uncertainties, u_T , are 0.34% (365nm) and 0.28% (UVA) according to equation (6.3.1). The transfer uncertainties of CSIR's results are summarized in Table 7.3.3b.

Table 7.3.3b Transfer uncertainty of CSIR's results

	365nm	UVA
u_{drift} (%)	0.08	0.08
u_{stab} (%)	0.33	0.27
u_T (%)	0.34	0.28

7.3.4 Comparison with the pilot lab reference value

The corrected relative difference Δ in the comparison was calculated for each detector, according to the equation (5.2.1) in the section 5.2, as shown in table 7.3.4.

*Note: CSIR has changed its data of calibration result for *s*(UVA) on 26 September 2005.*

Table 7.3.4a Relative difference in the comparison ($s_{CSIR} - s_{SPRING}$)/ s_{SPRING}

Detector (s/n)	Δ_3 (%), 365nm	Δ_3 (%), UVA
7108	+6.44	+8.04
7112	+6.91	+8.45
Average	+6.68	+8.24

The combined relative standard uncertainty of the comparison $u(\Delta_3)$ is calculated according to following formula (7.3.4) and summarized in the table 7.3.4b.

$$u^2(\Delta_3) = u_{rel}^2(\Delta_3) + u_T^2(\Delta_3) \quad (7.3.4)$$

$u_{rel}(\Delta_i)$: Total relative uncertainty of $s(365)$ or $s(UVA)$ reported by the participant.

$u_T(\Delta_i)$: The transfer uncertainty due to drift of transfer detectors and the stability of the comparison scale.

Table 7.3.4b Combined relative standard uncertainty of CSIR results ($k=1$)

	365nm	UVA
$u_{rel}(\Delta_3), \%$	4.0	7.5
$u_T(\Delta_3), \%$	0.34	0.28
$u(\Delta_3), \%$	4.01	7.51

7.4 ITRI (Chinese Taipei)

7.4.1 Measurement conditions and methods

a) Measurement conditions

- Spectroradiometer type: Bentham M300HR/2 double monochromator
- Standards used: Pyroelectric radiometer for $s(365)$ and $s(UVA)$
- Irradiance level: 0.1 mW/cm² (365nm), 0.6mW/cm² (UVA)
- Room temperature: 23.0 ± 1.5 °C
- Aperture diameter of standard detector: Φ11.3mm (0.9915cm²) (Absolute radiometer), Φ11.3mm (1.0cm²) (Pyroelectric radiometer)

b) Method used to determine $s(UVA)$ of transfer detector

$s(UVA)$ of transfer detector was calculated according to equation (5.1.1) through measurements of relative spectral irradiance of the comparison UV source and absolute spectral responsivity, $s(\lambda)$, of the transfer detector. $s(\lambda)$ of the transfer detector was determined by measuring its relative spectral responsivity in UVA range and calibrating its absolute responsivity at 365 nm.

c) Method used to determine $s(365)$ of transfer detector

$s(365)$ of transfer detector was calibrated by comparison with the absolute radiometer and pyroelectric radiometer against the comparison UV source with a UV (365nm) filter.

7.4.2 Uncertainty budget

Table 7.4.2a and 7.4.2b are the uncertainty budgets of calibration of transfer detectors under narrow band UV (365nm) and broad band UVA irradiance ($k=1$).

Table 7.4.2a Uncertainty budget of $s(365)$ of transfer detectors ($k=1$)

	Source of uncertainty	Value of standard uncertainty (%)
1	Calibration of standard detector	1.0
2	Photocurrent measurement	0.01
3	Reading repeatability of standard detector	0.5
4	Reading repeatability of test detector	0.5
5	Alignment and positioning of standard detector	0.2
6	Alignment and positioning of test detector	0.2
7	Uncertainty due to uniformity of UV beam and area difference between standard & test detectors	0.2
8	Others (please specify)	
	Combined relative standard uncertainty (%)	1.3

Table 7.4.2b Uncertainty budget of $s(UVA)$ of transfer detectors ($k=1$)

	Source of uncertainty	Value of standard uncertainty (%)
1	Calibration of standard detector	1.2
2	Photocurrent measurement	0.01
3	Reading repeatability of standard detector	0.7
4	Reading repeatability of test detector	0.3
5	Alignment and positioning of standard detector	0.2
6	Alignment and positioning of test detector	0.2
7	Uncertainty due to uniformity of UV beam and area difference between std & test detectors	0.2
8	Others (please specify)	
	Combined relative standard uncertainty (%)	1.5

7.4.3 Correction factors and transfer uncertainty

a) Correction

- Temperature: 23+/-1.5°C (No correction has been applied)
- Irradiance levels measured in ITRI are 0.1 mW/cm² (365nm) and 0.6mW/cm² (UVA). The correction factors are 1.000679 for $s(365)$ and 1.001174 for $s(UVA)$.

The correction for the different measurement condition is summarized in the table 7.4.3a.

Table 7.4.3a Correction for different measurement conditions with pilot lab

	$s(365)$		$s(UVA)$	
Correction factor	1.000679		1.001174	
Detector s/n	7108	7112	7108	7112
Before correction	0.00767	0.00797	0.00580	0.00599
After correction	0.007675	0.007975	0.005807	0.006004

b) Transfer uncertainty

Drifts of $s(365)$ and $s(UVA)$ before and after measurement in ITRI are 1.1% and 0.01% respectively. The standard uncertainties due to drifts of $s(365)$ and $s(UVA)$ of transfer detectors, u_{drift} , are 0.32% and 0.003% respectively according to equation (6.1.1). The standard uncertainties due to stability of the comparison scale, u_{stab} , are 0.33% (365nm) and 0.27% (UVA) according to equation (6.2.1). The transfer uncertainties, u_T , are 0.46% (365nm) and 0.27% (UVA) according to equation (6.3.1). The transfer uncertainties of ITRI's results are summarized in Table 7.4.3b.

Table 7.4.3b Transfer uncertainty of ITRI's results

	365nm	UVA
$u_{drift} (\%)$	0.32	0.003
$u_{stab} (\%)$	0.33	0.27
$u_T (\%)$	0.46	0.27

7.4.4 Comparison with pilot lab reference value

The corrected relative difference Δ in the comparison was calculated for each detector, according to the equation (5.2.1) in the section 5.2, as shown in table 7.4.4a.

Table 7.4.4a Relative difference in the comparison ($s_{ITRI} - s_{SPRING}$)/ s_{SPRING}

Detector (s/n)	$\Delta_4 (\%), 365nm$	$\Delta_4 (\%), UVA$
7108	+3.90	+3.91
7112	+5.14	+4.70
Average	+4.52	+4.31

The combined relative standard uncertainty of the comparison $u(\Delta_4)$ is calculated according to following formula (7.4.4) and summarized in the table 7.4.4.

$$u^2(\Delta_4) = u_{rel}^2(\Delta_4) + u_T^2(\Delta_4) \quad (7.4.4)$$

$u_{rel}(\Delta_i)$: Total relative uncertainty of $s(365)$ or $s(UVA)$ reported by the participant.

$u_T(\Delta_i)$: The transfer uncertainty due to drift of transfer detectors and the stability of the comparison scale.

Table 7.4.4b Combined relative standard uncertainty of ITRI results ($k=1$)

	365nm	UVA
$u_{rel}(\Delta_i)$	1.3	1.5
$u_T(\Delta_i)$	0.46	0.27
$u(\Delta_i)$	1.38	1.52

7.5 KRISS (South Korea)

7.5.1 Measurement conditions and methods

a) Measurement conditions

- Spectroradiometer type: Mcpherson 2061, 1m, prism+grating monochromator
- Standards used: ECPR for s(365) and standard lamps for s(UVA)
- Irradiance level: 0.16 mW/cm² (365nm), 0.98mW/cm² (UVA)
- Room temperature: 23.0 ± 0.5 °C
- Aperture diameter of standard detector: Φ8mm (ECPR), Φ18mm (Spectroradiometer)

b) Method used to determine s(UVA) of transfer detector

s(UVA) of transfer detector was calibrated by measuring the output signal of the transfer detector against UVA irradiance of the comparison UV source whose spectral irradiance was calibrated by reference standard spectral irradiance lamps maintained in KRISS.

c) Method used to determine s(365) of transfer detector

s(365) of transfer detector was calibrated by comparison with a reference standard ECPR against the comparison UV source with a UV(365nm) filter.

7.5.2 Uncertainty budget

Table 7.5.2a and 7.5.2b are the uncertainty budgets of calibration of transfer detector under narrow band UV (365nm) and broad band UVA irradiance ($k=1$).

Table 7.5.2a Uncertainty budget of s(365) of transfer detector ($k=1$)

	Source of uncertainty	Value of standard uncertainty (%)
1	Calibration of standard detector	0.56
2	Photocurrent measurement	0.02
3	Reading repeatability of standard detector	0.19
4	Reading repeatability of test detector	0.25
5	Alignment and positioning of standard detector	0.17
6	Alignment and positioning of test detector	0.17
7	Uncertainty due to uniformity of UV beam and area difference between standard & test detectors	0.03
8	Others (please specify)	
	Combined relative standard uncertainty (%)	0.68

Table 7.5.2b Uncertainty budget of $s(UVA)$ of transfer detector ($k=1$)

	Source of uncertainty	Value of standard uncertainty (%)
1	Calibration of standard detector	1.69
2	Photocurrent measurement	0.02
3	Reading repeatability of test detector	0.25
4	Alignment and positioning of test detector	0.17
5	Uncertainty due to uniformity of UV beam and area difference between std & test detectors	0.03
6	Others (please specify)	
	Combined relative standard uncertainty (%)	1.72

7.5.3 Measurement conditions and transfer uncertainty

a) Correction

- Temperature: 23 \pm 0.5°C (No correction applied)
- Irradiance levels measured in KRISS are 0.16 mW/cm² (365nm) and 0.98mW/cm² (UVA). The UV irradiance levels are similar with those in the pilot lab and no correction has been applied.

b) Transfer uncertainty

Drifts of $s(365)$ and $s(UVA)$ before and after measurement in KRISS are -0.85% and 0.09% respectively. The standard uncertainties due to drifts of $s(365)$ and $s(UVA)$ of transfer detectors, u_{drift} , are 0.25% and 0.03% respectively according to equation (6.1.1). The standard uncertainties due to stability of the comparison scale, u_{stab} , are 0.33% (365nm) and 0.27% (UVA) according to equation (6.2.1). The transfer uncertainties, u_T , are 0.41% (365nm) and 0.27% (UVA) according to equation (6.3.1). The transfer uncertainties of KRISS's results are summarized in Table 7.5.3.

Table 7.5.3 Transfer uncertainty of KRISS's results

	365nm	UVA
u_{drift} (%)	0.25	0.03
u_{stab} (%)	0.33	0.27
u_T (%)	0.414	0.27

7.5.4 Comparison with the pilot lab reference value

The corrected relative difference Δ in the comparison was calculated for each detector, according to the equation (5.2.1) in the section 5.2, as shown in table 7.5.4a.

Table 7.5.4a Relative difference in the comparison $(s_{\text{KRISS}} - s_{\text{SPRING}})/s_{\text{SPRING}}$

Detector (s/n)	Δ_5 (%), 365nm	Δ_5 (%), UVA
7108	-0.32	-2.87
7112	-0.13	-2.91
Average	-0.22	-2.89

The combined relative standard uncertainty of the comparison $u(\Delta_5)$ is calculated according to following formula (7.5.4) and summarized in the table 7.5.4b.

$$u^2(\Delta_5) = u_{rel}^2(\Delta_5) + u_T^2(\Delta_5) \quad (7.5.4)$$

$u_{rel}(\Delta_i)$: Total relative uncertainty of $s(365)$ or $s(\text{UVA})$ reported by the participant.

$u_T(\Delta_i)$: The transfer uncertainty due to drift of transfer detectors and the stability of the comparison scale.

Table 7.5.4b Combined relative standard uncertainty of KRISS results ($k=1$)

	365nm	UVA
$u_{rel}(\Delta_5)$, %	0.68	1.72
$u_T(\Delta_5)$, %	0.414	0.27
$u(\Delta_5)$, %	0.80	1.74

7.6 NIM (China)

7.6.1 Measurement conditions and methods

a) Measurement conditions

- Spectroradiometer: type a) Single grating monochromator + PTFE integrating sphere + diffuser (made in China). Type b) SPECTRO 320 Single grating monochromator + PTFE integrating sphere + diffuser (made in Germany)
- Standards used: standard lamps for $s(365)$ and $s(\text{UVA})$
- Irradiance level: 0.133-0.143 mW/cm² (365nm), 0.578-0.895mW/cm² (UVA)
- Room temperature: 21-24 °C
- Aperture diameter of spectroradiometer: $\Phi 28.5$ mm (type a), $\Phi 21$ mm (type b)

b) Method used to determine $s(\text{UVA})$ of transfer detector

$s(\text{UVA})$ of transfer detector was calibrated by measuring the output signal of the transfer detector against UVA irradiance of the comparison UV source whose spectral irradiance was calibrated by reference standard spectral irradiance lamps maintained in NIM.

c) Method used to determine $s(365)$ of transfer detector

$s(365)$ of transfer detector was calibrated by measuring the output signal of the transfer detector against the irradiance of the comparison UV source with a UV (365nm) filter

whose spectral irradiance was calibrated by reference standard spectral irradiance lamps maintained in NIM.

7.6.2 Uncertainty budget

Table 7.6.2a and 7.6.2b are the uncertainty budgets of calibration of transfer detector under narrow band UV (365nm) and broad band UVA irradiance ($k=1$).

Table 7.6.2a Uncertainty budget of $s(365)$ of transfer detector

No.	Source of uncertainty	Value of standard uncertainty (%)	Type
1	Measurement repeatability of the photocurrent	0.20	A
2	Measurement repeatability of the UVA integral irradiance	1.20	A
3	Uncertainty of the standard lamp group of spectral irradiance	0.58	B
4	Alignment and positioning of the spectral irradiance standard lamp	0.20	B
5	Current measurement of the standard lamp	0.10	B
6	Distance measurement of the standard lamp	0.50	B
7	Aging of the standard lamp	0.10	B
8	Wavelength accuracy and repeatability of the spectroradiometer	0.50	B
9	Alignment and positioning of the spectroradiometer	0.10	B
10	Instability of the spectroradiometer	0.23	B
11	Short term stability of the UV source during measurement	0.23	B
12	Alignment and positioning of the UV source	0.10	B
13	Uncertainty due to Non-uniformity of the UV beam and area difference between the spectroradiometer and the UVA detector for comparison	0.20	B
14	Alignment and positioning of the UV(365) filter	0.80	B
15	Alignment and positioning of the detector for comparison	0.50	B
16	Stray radiation	1.00	B
17	Non-linearity of measurement system	0.10	B
18	Uncertainty of the I/V converter	0.10	B
19	Uncertainty of the 6 1/2 digit multimeter	0.01	B
Combined relative standard uncertainty (%)		2.1	

Table 7.6.2b Uncertainty budget of $s(UVA)$ of transfer detector

No.	Source of uncertainty	Value of standard uncertainty (%)	Type
1	Measurement repeatability of the photocurrent	0.20	A
2	Measurement repeatability of the UVA integral irradiance	1.20	A
3	Uncertainty of the standard lamp group of spectral irradiance	0.58	B
4	Alignment and positioning of the spectral irradiance standard lamp	0.20	B
5	Current measurement of the standard lamp	0.10	B
6	Distance measurement of the standard lamp	0.50	B
7	Aging of the standard lamp	0.10	B
8	Wavelength accuracy and repeatability of the spectroradiometer	0.50	B
9	Alignment and positioning of the spectroradiometer	0.10	B
10	Repeatability of the spectroradiometer	0.23	B
11	Short term stability of the UV source during measurement	0.23	B
12	Alignment and positioning of the UV source	0.10	B
13	Uncertainty due to Non-uniformity of the UV beam and area difference between the spectroradiometer and the UVA detector for comparison	0.20	B
14	Alignment and positioning of the detector for comparison	0.50	B
15	Stray radiation	1.00	B
16	Non-linearity of measurement system	0.10	B
17	Uncertainty of the I/V converter	0.10	B
18	Uncertainty of the 6 1/2 digit multimeter	0.01	B
Combined relative standard uncertainty (%)		2.0	

7.6.3 Correction factors and transfer uncertainty

a) Correction

- Temperature: 21-23°C (365) and 21-24°C (UVA). The correction factors are 0.999696 for $s(365)$ for average temperature of 22°C and 0.999323 for $s(UVA)$ according to the average temperature at 22.5°C.
- Irradiance levels are 0.133-0.143 mW/cm² (365nm) and 0.578-0.895mW/cm² (UVA). As the irradiance levels are similar with those in the pilot lab, no correction has been applied.

The correction for the different measurement condition is summarized in the table 7.6.3a.

Table 7.6.3a Correction for different measurement conditions with pilot lab

	<i>s</i> (365)		<i>s</i> (UVA)	
Correction factor	0.999696		0.999323	
Detector s/n	7108	7112	7108	7112
Before correction	0.00737	0.00764	0.00560	0.00577
After correction	0.007368	0.007638	0.005596	0.005766

b) Transfer uncertainty

Drifts of *s*(365) and *s*(UVA) before and after measurement in NIM are -0.19% and -0.26% respectively. The standard uncertainties due to drifts of *s*(365) and *s*(UVA) of transfer detectors, u_{drift} , are 0.05% and 0.08% respectively according to equation (6.1.1). The standard uncertainties due to stability of the comparison scale, u_{stab} , are 0.33% (365nm) and 0.27% (UVA) according to equation (6.2.1). The transfer uncertainties, u_T , are 0.33% (365nm) and 0.28% (UVA) according to equation (6.3.1). The transfer uncertainties of NIM's results are summarized in Table 7.6.3b.

Table 7.6.3b Transfer uncertainty of NMI's results

	365nm	UVA
u_{drift} (%)	0.05	0.08
u_{stab} (%)	0.33	0.27
u_T (%)	0.33	0.28

7.6.4 Comparison with the pilot lab reference value

The corrected relative difference Δ in the comparison was calculated for each detector, according to the equation (5.2.1) in the section 5.2, as shown in table 7.6.4a.

Note: NIM has repeated its measurements to eliminate previously undetected errors. The data provided is the second calibration results.

Table 7.6.4a Relative difference in the comparison $(s_{NIM} - s_{SPRING})/s_{SPRING}$

Detector (s/n)	Δ_6 (%), 365nm	Δ_6 (%), UVA
7108	+1.03	+0.32
7112	+0.68	+0.06
Average	+0.86	+0.19

The combined relative standard uncertainty of the comparison $u(\Delta_6)$ is calculated according to following formula (7.6.4) and summarized in the table 7.6.4b.

$$u^2(\Delta_6) = u_{rel}^2(\Delta_6) + u_T^2(\Delta_6) \quad (7.6.4)$$

$u_{rel}(\Delta_i)$: Total relative uncertainty of *s*(365) or *s*(UVA) reported by the participant.

$u_T(\Delta_i)$: The transfer uncertainty due to drift of transfer detectors and the stability of the comparison scale.

Table 7.6.4b Combined relative standard uncertainty of NIM results ($k=1$)

	365nm	UVA
$u_{rel}(\Delta_6), \%$	2.1	2.0
$u_T(\Delta_6), \%$	0.33	0.28
$u(\Delta_6), \%$	2.13	2.02

8. Overall Results

8.1. Agreement among laboratories

As all the results from national laboratories have been compared with the SPRING Singapore calibrations, the latter being used as a reference, it is possible to calculate the difference between the results of any two participants and check if they agree within the uncertainties of the comparison. The results of these calculations, using the standard uncertainty ($k=1$), are shown in Table 8.1.1, Figures 8.1.1 and 8.1.2.

Table 8.1.1 Relative difference (Δ_i) from SPRING Singapore reference value and combined uncertainty, $u(\Delta_i)$

i	NMI	365nm		UVA	
		$\Delta_i(\%)$	$u(\Delta_i)(\%, k=1)$	$\Delta_i(\%)$	$u(\Delta_i)(\%, k=1)$
0	SPRING	0	1.60	0	2.40
1	NMIA	0.60	1.15	-0.17	0.47
2	NMIJ	2.41	1.64	2.73	3.21
3	CSIR	6.68	4.01	8.24	7.51
4	ITRI	4.52	1.38	4.31	1.52
5	KRISS	-0.22	0.80	-2.89	1.74
6	NIM	0.86	2.13	0.19	2.02

*Note: Mark * indicates the lab has repeated its measurements to eliminate previously undetected errors.*

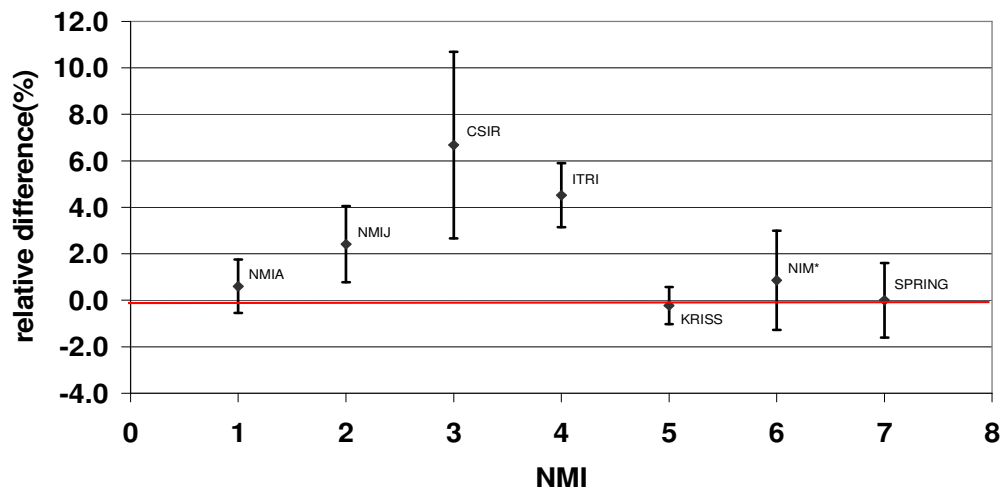


Fig.8.1.1 Relative difference and combined uncertainty ($k=1$) of $s(365)$ against the SPRING Singapore reference value

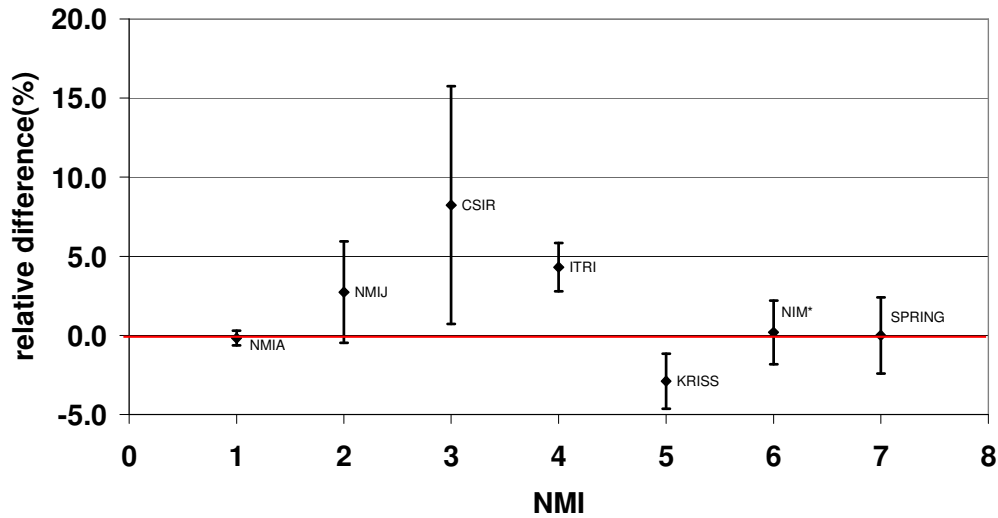


Fig. 8.1.2 Relative difference and combined uncertainty ($k=1$) of $s(UVA)$ against the SPRING Singapore reference value

8.2 Comparison with comparison reference value

8.2.1 Calculation of comparison reference value ^[11.9]

According to “Guidelines for CCPR Comparison Report Preparation, Rev.1, March 2006”, the default method for calculating KCRV is the weighted mean with cut-off. This comparison adopts the same method to calculate the comparison reference value (CRV).

The cut-off value for the uncertainty, as a default, is determined as the average of the uncertainty values of those participants that reported uncertainties smaller than or equal to the median of all the participants as shown in equation (8.2.1).

$$u_{cut-off} = \text{average}\{u_{rel}(\Delta_i)\} \text{ for } u_{rel}(\Delta_i) \leq \text{median}\{u_{rel}(\Delta_i)\}; i=0 \text{ to } N \quad (8.2.1)$$

where $N(=6)$ is number of participant NMIs, not counting the pilot lab.

In this comparison, the cut-off value, $u_{cut-off}$, is the average of the 4 smallest values of uncertainty.

The relative differences of participants from pilot lab reference value and reported uncertainty value are summarized in table 8.2.1.

Table 8.2.1 Relative difference (Δ_i) from SPRING Singapore reference value and reported uncertainty, $u_{rel}(\Delta_i)$

i	NMI	365nm		UVA	
		Δ_i (%)	$u_{rel}(\Delta_i)$ (%)	Δ_i (%)	$u_{rel}(\Delta_i)$ (%)
0	SPRING	0	1.6	0	2.4
1	NMIA	0.60	1.1	-0.17	0.29
2	NMIJ	2.41	1.6	2.73	3.2
3	CSIR	6.68	4.0	8.24	7.5
4	ITRI	4.52	1.3	4.31	1.5
5	KRISS	-0.22	0.68	-2.89	1.72
6	NIM	0.86	2.1	0.19	2.0

According to Table 8.2.1, median $\{u_{rel}(\Delta_i)\}$ are 1.6% (365nm) and 2.0% (UVA) respectively.

Therefore, $u_{cut-off}$ are 1.17% (365nm) and 1.38% (UVA) respectively.

The reported uncertainties $u_{rel}(\Delta_i)$ of each NMI (i) are adjusted by the cut-off according to following equations(8.2.2a – 8.2.3b).

For 365nm,

$$u_{rel,adj}(\Delta_i) = u_{rel}(\Delta_i) \quad \text{for } u_{rel}(\Delta_i) \geq 1.17\% \quad (8.2.2a)$$

$$u_{rel,adj}(\Delta_i) = 1.17\% \quad \text{for } u_{rel}(\Delta_i) < 1.17\% \quad (8.2.2b)$$

For UVA,

$$u_{rel,adj}(\Delta_i) = u_{rel}(\Delta_i) \quad \text{for } u_{rel}(\Delta_i) \geq 1.38\% \quad (8.2.3a)$$

$$u_{rel,adj}(\Delta_i) = 1.38\% \quad \text{for } u_{rel}(\Delta_i) < 1.38\% \quad (8.2.3b)$$

The uncertainties of NMIs before and after adjustment are listed in table 8.2.2.

Table 8.2.2 Uncertainties of NMIs before and after adjustment

i	NMI	365nm		UVA	
		$u_{rel}(\Delta_i)$	$u_{rel,adj}(\Delta_i)$	$u_{rel}(\Delta_i)$	$u_{rel,adj}(\Delta_i)$
0	SPRING	1.6	1.6	2.4	2.4
1	NMIA	1.1	1.17	0.29	1.38
2	NMIJ	1.6	1.6	3.2	3.2
3	CSIR	4.0	4.0	7.5	7.5
4	ITRI	1.3	1.3	1.5	1.5
5	KRISS	0.68	1.17	1.72	1.72
6	NIM	2.1	2.1	2.0	2.0

The transfer uncertainties of participants are listed in table 8.2.3 according to the data obtained from each participant in Chapter 7.

As the uncertainty due to the stability of SPRING's comparison scale was included in the relative standard uncertainty, $u_{rel}(\Delta_i)$, of SPRING's measurements and the drift of $s(365)$ and $s(UVA)$ of transfer detectors are not applicable to SPRING, the transfer uncertainties of SPRING's measurements are zero in the table 8.2.3.

Table 8.2.3 Summary of transfer uncertainty, $u_T(\Delta_i)$

i	NMI	365nm	UVA
0	SPRING	0	0
1	NMIA	0.33	0.37
2	NMIJ	0.34	0.29
3	CSIR	0.34	0.28
4	ITRI	0.46	0.27
5	KRISS	0.41	0.27
6	NIM	0.33	0.28

The uncertainty of Δ_i after cut-off is given by using equation (8.2.4) and listed in table 8.2.4

$$u_{adj}(\Delta_i) = \sqrt{u_{rel,adj}^2(i) + u_T^2(\Delta_i)} \tag{8.2.4}$$

Table 8.2.4 Summary of $u_{adj}(\Delta_i)$

i	NMI	365nm			UVA		
		$u_T(\Delta_i)$	$u_{rel,adj}(\Delta_i)$	$u_{adj}(\Delta_i)$	$u_T(\Delta_i)$	$u_{rel,adj}(\Delta_i)$	$u_{adj}(\Delta_i)$
0	SPRING	0	1.6	1.60	0	2.4	2.40
1	NMIA	0.33	1.17	1.22	0.37	1.38	1.43
2	NMIJ	0.34	1.6	1.64	0.29	3.2	3.21
3	CSIR	0.34	4.0	4.01	0.28	7.5	7.51
4	ITRI	0.46	1.3	1.38	0.27	1.5	1.52
5	KRISS	0.41	1.17	1.24	0.27	1.72	1.74
6	NIM	0.33	2.1	2.13	0.28	2.0	2.02

The weights w_i for NMI i is determined by using equation (8.2.5) and listed in table 8.2.5.

$$w_i = u_{adj}^{-2}(\Delta_i) / \sum_{i=0}^N u_{adj}^{-2}(\Delta_i) \tag{8.2.5}$$

Table 8.2.5 Calculation of the weights

i	NMI	365nm		UVA	
		$u_{adj}^{-2}(\Delta_i)$	w_i	$u_{adj}^{-2}(\Delta_i)$	w_i
0	SPRING	0.391	0.135	0.174	0.097
1	NMIA	0.676	0.233	0.490	0.275
2	NMIJ	0.373	0.129	0.097	0.054
3	CSIR	0.062	0.021	0.018	0.010
4	ITRI	0.526	0.181	0.430	0.241
5	KRISS	0.649	0.224	0.330	0.185
6	NIM	0.221	0.076	0.245	0.137
	sum	2.898		1.784	

The comparison reference value (CRV), Δ_{CRV} , is determined by using equation (8.2.6) and listed in table 8.2.6.

$$\Delta_{CRV} = \sum_{i=0}^N w_i \Delta_i \tag{8.2.6}$$

Table 8.2.6 Calculation of CRV, Δ_{CRV}

i	NMI	365nm			UVA		
		w_i	Δ_i	$w_i \Delta_i$	w_i	Δ_i	$w_i \Delta_i$
0	SPRING	0.135	0	0	0.097	0	0
1	NMIA	0.233	0.60	0.140	0.275	-0.17	-0.047
2	NMIJ	0.129	2.41	0.310	0.054	2.73	0.148
3	CSIR	0.021	6.68	0.143	0.010	8.24	0.082
4	ITRI	0.181	4.52	0.820	0.241	4.31	1.040
5	KRISS	0.224	-0.22	-0.049	0.185	-2.89	-0.534
6	NIM	0.076	0.86	0.066	0.137	0.19	0.026
	Δ_{CRV}			1.430			0.715

8.2.2 Uncertainty associated with the comparison reference value

The uncertainty of the CRV (weighted mean with cut-off) is determined by using equation (8.2.7).

$$u(\Delta_{CRV}) = \sqrt{\sum_{i=0}^N \frac{u^2(\Delta_i)}{u_{adj}^4(\Delta_i)} \bigg/ \sum_{i=0}^N u_{adj}^{-2}(\Delta_i)} \tag{8.2.7}$$

The uncertainty values of the CRV, $u(\Delta_{CRV})$ are **0.54%** (365nm) and **0.65%** (UVA).

8.2.3 Unilateral degree of equivalence of NMIs

The unilateral DoE of a NMI is given by

$$D_i = \Delta_i - \Delta_{CRV} \tag{8.2.8}$$

$$U_i = k \sqrt{u^2(\Delta_i) + u^2(\Delta_{CRV}) - 2 \left[\frac{u^2(\Delta_i)}{u_{adj}^2(\Delta_i)} \bigg/ \sum_{j=0}^N u_{adj}^{-2}(\Delta_j) \right]} \quad (k = 2) \tag{8.2.9}$$

The results of unilateral degree of equivalence of NMIs are listed in table 8.2.7 and shown in Figure 8.2.1 and 8.2.2.

Table 8.2.7 The unilateral degree of equivalence of NMIs

i	NMI	365nm		UVA	
		$D_i(\%)$	$U_i(\%, k=2)$	$D_i(\%)$	$U_i(\%, k=2)$
0	SPRING	-1.43	2.94	-0.72	4.50
1	NMIA	-0.83	2.00	-0.89	1.44
2	NMIJ	0.98	3.02	2.01	6.20
3	CSIR	5.25	7.93	7.52	14.92
4	ITRI	3.09	2.45	3.59	2.55
5	KRISS	-1.65	1.60	-3.61	3.06
6	NIM	-0.57	4.06	-0.53	3.68

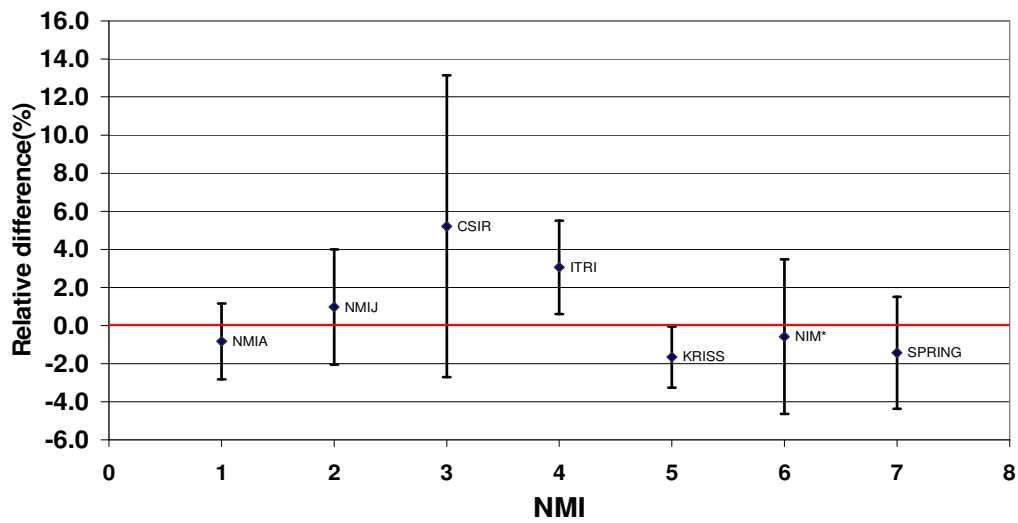


Fig. 8.2.1 Relative difference and combined uncertainty ($k=2$) of $s(365)$ against the comparison weighted mean with cut-off

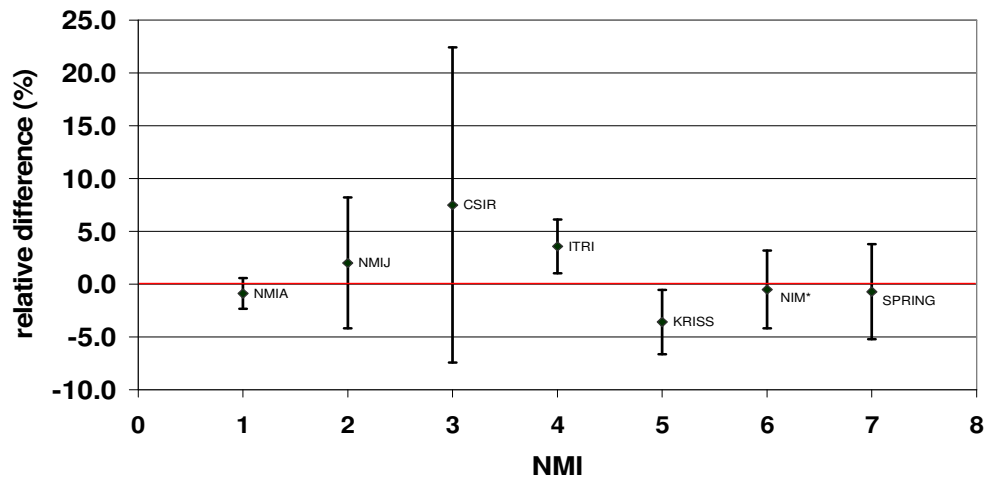


Fig. 8.2.2 Relative difference and combined uncertainty ($k=2$) of $s(UVA)$ against the comparison weighted mean with cut-off

8.2.4 Bilateral degree of equivalence between NMIs

The bilateral DoE between NMI(i) and NMI(m) is given by

$$D_{i,m} = \Delta_i - \Delta_m \quad (8.2.10)$$

$$U_{i,m} = k\sqrt{u^2(\Delta_i) + u^2(\Delta_m)} \quad ; \quad k = 2 \quad (8.2.11)$$

The results of relative difference between NMIs and their relative uncertainty for 365nm and UVA are listed in table 8.2.8 – 8.2.11.

Table 8.2.8 Relative difference between NMIs for 365nm

D_{im}(365)%	NMIA	NMIJ	CSIR	ITRI	KRISS	NIM
NMIJ	1.81					
CSIR	6.08	4.27				
ITRI	3.92	2.11	-2.16			
KRISS	-0.82	-2.63	-6.90	-4.74		
NIM	0.26	-1.55	-5.82	-3.66	1.08	
SPRING	-0.60	-2.41	-6.68	-4.52	0.22	-0.86

Table 8.2.9 Relative uncertainty of D_{im} (365),(k=2)

U_{im}(365)%	NMIA	NMIJ	CSIR	ITRI	KRISS	NIM
NMIJ	3.62					
CSIR	8.18	8.48				
ITRI	3.16	3.89	8.30			
KRISS	2.56	3.42	8.09	2.93		
NIM	4.52	5.06	8.91	4.74	4.36	
SPRING	3.55	4.21	8.46	3.83	3.35	5.01

Table 8.2.10 Relative difference between NMIs for UVA

D_{im}(UVA)%	NMIA	NMIJ	CSIR	ITRI	KRISS	NIM
NMIJ	2.90					
CSIR	8.41	5.51				
ITRI	4.48	1.58	-3.93			
KRISS	-2.72	-5.62	-11.13	-7.20		
NIM	0.36	-2.54	-8.05	-4.12	3.08	
SPRING	0.17	-2.73	-8.24	-4.31	2.89	-0.19

Table 8.2.11 Relative uncertainty of D_{im} (UVA), (k=2)

U_{im}(UVA)%	NMIA	NMIJ	CSIR	ITRI	KRISS	NIM
NMIJ	6.37					
CSIR	14.99	16.16				
ITRI	2.93	6.71	15.13			
KRISS	3.38	6.92	15.23	3.98		
NIM	3.95	7.21	15.36	4.47	4.78	
SPRING	4.73	7.66	15.58	5.17	5.44	5.81

8.2.5 Statistical checks

The overall consistency of the actual dispersion with the uncertainties is checked by means of Chi-Squared test.

The observed chi-squared value is formed with:

$$\chi_{obs}^2 = \sum_{i=1}^N \frac{\left(\frac{\Delta_i - \Delta_{CRV}}{\Delta_{CRV}} \right)^2}{u_i^2} \quad (8.2.12)$$

where N is the number of independent results.

The degrees of freedom depend on the number of independent results: $\nu = N-1=6$.

The Chi-Squared test was carried out according to data provided in table 8.2.7 and results were summarized in table 8.2.12 (See detail of calculation in Appendix 1). The results indicated the consistency check is ok as $X^2(\nu)$ value shown in the 0.05 column in the table of cumulative distribution of Chi-Squared ^[11.11] is greater than the observed Chi-Squared value (χ_{obs}^2).

Table 8.2.12 Chi-square test for the comparison results

	365nm	UVA
χ_{obs}^2	3.37	9.52
$X^2(\nu), \nu=6$	12.56	12.56
Consistency check: ok, if $X^2(6) > \chi_{obs}^2$	ok	ok

The consistency is also confirmed by the Birge ratio ^[11.12] formed with the ratio of the external consistency to the internal consistency, as follows:

- Internal consistency:

$$u_{int}^2 = \frac{1}{\sum_{i=1}^N u_i^{-2}} \quad (8.2.13)$$

- External consistency:

$$u_{ext}^2 = \frac{\sum \left(\left(\frac{\Delta_i - \Delta_{CRV}}{\Delta_{CRV}} \right)^2 \cdot u_i^{-2} \right)}{(N-1) \cdot \sum_{i=1}^N u_i^{-2}} \quad (8.2.14)$$

- Birge ratio:

$$R_B = \frac{u_{ext}}{u_{int}} \quad (8.2.15)$$

The Birge ratio for the weighted mean with cut-off presented in Table 8.2.13 leads to the same result as the chi-squared test, as R_B for UVA and 365nm are reasonably close to 1. (See detail of calculation in Appendix 2)

Table 8.2.13 Birge ratio test for the comparison results

	365nm	UVA
u_{int}	0.95	1.06
u_{ext}	0.79	1.20
R_B	0.83	1.13
Consistency check: ok, if R_B is close to 1.	ok	ok

9 Conclusion

The comparison results show most of the results lie within $\pm 5\%$ against the weighted mean with cut-off with a few exceptions.

The degree of agreement of such comparison depends not only on the base scales of spectral responsivity and spectral irradiance of a laboratory, but also equally important on the method used for such measurement. A number of major uncertainty sources have been identified for discrepancies observed in the comparison (e.g. the uncertainty caused by stray light in the measurement of spectral irradiance or spectral power distribution of UV source etc.).

This comparison also allowed some labs to improve their experimental method and arrangement so as to eliminate previous undetected errors.

10 Acknowledgements

The pilot lab wishes to thank the following colleagues from all participating labs:

Mark Ballico, Frank Wilkinson and Thorvaldson Erik (NMIA, Australia)
 Saito Terubumi (NMIJ, Japan)
 LAG Monard (CSIR, South Africa)
 Hsueh-Ling Yu (ITRI, Chinese Taipei)
 Dong-Joo Shin (KRISS, South Korea)
 Lin Yandong, Dai Caihong and Yu Jialin (NIM, China)

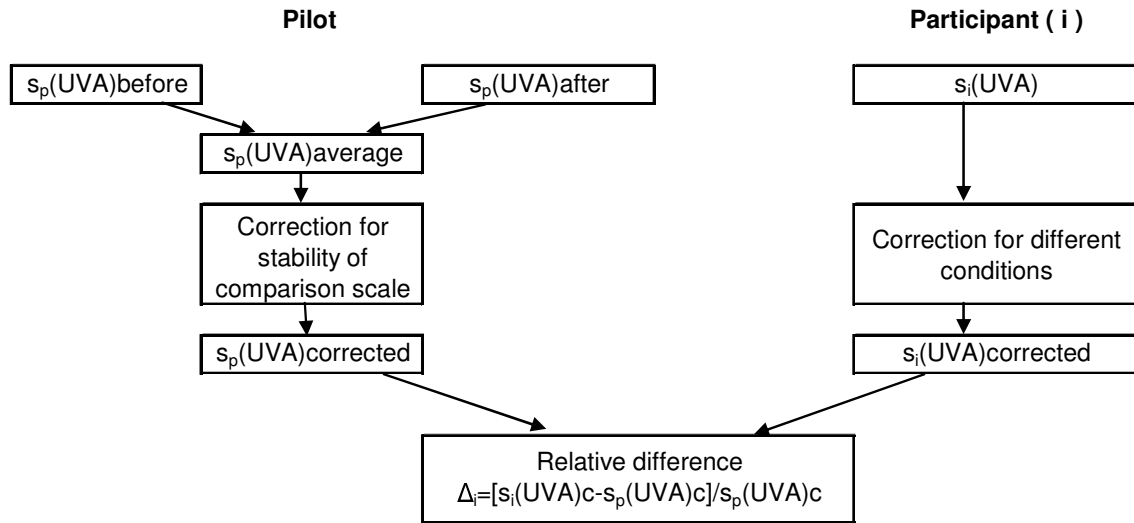
for their cooperation in the measurements and contribution of comments and feedback in the review of the report which enabled the comparison be completed smoothly.

11 References

- 11.1 SPRING Singapore, Technical protocol for APMP comparison on irradiance responsivity of UVA detectors, 26 Nov. 2002
- 11.2 G Xu and X Huang, Characterization and calibration of broadband ultraviolet radiometers, *Metrologia* 2000, 37, 235-242
- 11.3 G Xu, Methods of characterization and calibration of broadband UV radiometers, First draft, CIE TC2-47 document, 2001
- 11.4 G Xu and X Huang, Calibration of broadband UV radiometers - methodology and uncertainty evaluation, *Metrologia*, 40, (2003), S21- S24
- 11.5 X Huang, G Xu and Y Liu, Comparison of two calibration methods for UVA broadband detector, Proceedings on CIE Midterm Meeting and International Lighting Congress, LEON 2005
- 11.6 R. Goebel, M. Stock, and R. Köhler, Report on the international comparison of cryogenic radiometer based on transfer detectors, BIPM report, BIPM-2000/9
- 11.7 L. P. Boivin, Automated absolute and relative spectral linearity measurements on photovoltaic detectors, *Metrologia* 1993, 30,355-360
- 11.8 Guide to the Expression of Uncertainty in Measurement, First edition 1995 (ISO, 1995).
- 11.9 Guidelines for CCPR Comparison Report Preparation, CCPR Key Comparison Working Group, Rev.1, March 2006
- 11.10 Report on the key comparison CCPR-K2.b of spectral responsivity measurements in the wavelength range 300 nm to 1000 nm, BIPM (R. Goebel and M. Stock), October 2004
- 11.11 George W. Snedecor, *Statistical Methods*, Seventh Edition, P.470 (1980)
- 11.12 Taylor B.N., Parker W.H. and Langenberg D.N., *Rev. Mod. Phys.*, 1969, 41 (3), 3275-3496.

Appendix 1. Flowchart of data analysis for comparison results

(1) Flow chart of data analysis for comparison result of s(UVA) or s(365) of both transfer detectors



Note: Data analysis for s(365) is same as that of s(UVA)

Appendix 2. Statistical check for the consistency of the comparison results

(1) Chi-Squared test

Chi-Squared test for 365nm

	$\Delta_i(\%)$	$\Delta_{CRV}(\%)$	$u_i(\%)$	$[(\Delta_i/\Delta_{CRV}-1)/u_i]^2$
NMIA	-0.83	1.43	2.00	0.6273
NMIJ	0.98	1.43	3.02	0.0109
CSIR	5.25	1.43	7.93	0.1135
ITRI	3.09	1.43	2.45	0.2243
KRISS	-1.65	1.43	1.60	1.8099
NIM	-0.57	1.43	4.06	0.1186
SPRING	-1.43	1.43	2.94	0.4628
X_{obs}^2				3.3673
$X(v)^2=X(6)^2$				12.59

Consistency check: ok, if $X^2(6) > X_{obs}^2$

Chi-Squared test for UVA

	$\Delta_i(\%)$	$\Delta_{CRV}(\%)$	$u_i(\%)$	$[(\Delta_i/\Delta_{CRV}-1)/u_i]^2$
NMIA	-0.89	0.715	1.44	2.3999
NMIJ	2.01	0.715	6.20	0.0858
CSIR	7.52	0.715	14.92	0.4076
ITRI	3.59	0.715	2.55	2.4955
KRISS	-3.61	0.715	3.06	3.9107
NIM	-0.53	0.715	3.68	0.2225
SPRING	-0.72	0.715	4.50	0.1977
X_{obs}^2				9.5220
$X(v)^2=X(6)^2$				12.59

Consistency check: ok, if $X^2(6) > X_{obs}^2$

Notes:

- a) $\Delta_i(\%)$: relative difference of $s(365)$ or $s(UVA)$ against comparison weighted mean with cut-off
- b) $\Delta_{CRV}(\%)$: the reference value of the comparison weighted mean with cut-off
- c) $u_i(\%)$: the uncertainty associated with comparison weighted mean with cut-off
- d) X_{obs}^2 : the observed Chi-Squared value

$$X_{obs}^2 = \sum_{i=1}^N \frac{\left(\frac{\Delta_i - \Delta_{CRV}}{\Delta_{CRV}} \right)^2}{u_i^2}$$

where N is the number of independent results (here $N=7$)

- e) $X(v)^2$: Chi-Squared value in the table of Chi-Squared with $N-1$ degrees of freedom for probability = 0.05 (when $v=N-1=6$, $X(6)^2=12.59$)

(2) Birge ratio test

Birge ratio test for 365nm

	u_i	$1/u_i^2$	Δ_i	Δ_{CRV}	$[(\Delta_i/\Delta_{CRV}-1)/u_i]^2$	R_B
NMIA	2.00	0.251141	-0.83	1.43	0.6273	
NMIJ	3.02	0.109662	0.98	1.43	0.0109	
CSIR	7.93	0.015907	5.25	1.43	0.1135	
ITRI	2.45	0.166430	3.09	1.43	0.2243	
KRISS	1.60	0.390164	-1.65	1.43	1.8099	
NIM	4.06	0.060647	-0.57	1.43	0.1186	
SPRING	2.94	0.115696	-1.43	1.43	0.4628	
Sum		1.109646			3.3673	
u_{int}^2		0.901188		u_{ext}^2	0.6227	
u_{int}		0.95		u_{ext}	0.79	0.83

Consistency check: ok, if R_B is close to 1.

Birge ratio test for UVA

	u_i	$1/u_i^2$	Δ_i	Δ_{CRV}	$[(\Delta_i/\Delta_{CRV}-1)/u_i]^2$	R_B
NMIA	1.44	0.478974	-0.89	0.715	2.3999	
NMIJ	6.20	0.025974	2.01	0.715	0.0858	
CSIR	14.92	0.004494	7.52	0.715	0.4076	
ITRI	2.55	0.153859	3.59	0.715	2.4955	
KRISS	3.06	0.107105	-3.61	0.715	3.9107	
NIM	3.68	0.073937	-0.53	0.715	0.2225	
SPRING	4.50	0.049388	-0.72	0.715	0.1977	
Sum		0.893731			9.7197	
u_{int}^2		1.118905		u_{ext}^2	1.4478	
u_{int}		1.06		u_{ext}	1.20	1.13

Consistency check: ok, if R_B is close to 1.

Notes:

- a) Δ_i : relative difference of $s(365)$ or $s(UVA)$ against comparison weighted mean with cut-off
- b) u_i : the uncertainty associated with comparison weighted mean with cut-off
- c) Δ_{CRV} : the reference value of the comparison weighted mean with cut-off
- d) u_{int}^2 : internal consistency

$$u_{int}^2 = 1 / \sum_{i=1}^N u_i^{-2}$$

- e) u_{ext}^2 : external consistency

$$u_{ext}^2 = \frac{\sum_{i=1}^N \left(\frac{\Delta_i - \Delta_{CRV}}{\Delta_{CRV}} \right)^2 \cdot u_i^{-2}}{(N-1) \cdot \sum_{i=1}^N u_i^{-2}}$$

where N is the number of independent results (here $N=7$)

- f) Birge ratio: $R_B = u_{ext} / u_{int}$